A DISSERTATION

FOR THE DEGREE OF DOCTOR OF PHILOSOPHY

Anti-tumor Effects of the Tyrosine Kinase Inhibitor Rivoceranib in Canine Melanoma and Mammary Gland Tumor

개의 악성 흑색종 및 유선암에서 Tyrosine Kinase Inhibitor인 Rivoceranib의 항종양 효과

2020년 2월

서울대학교 대학원

수의학과 임상수의학 (수의내과학) 전공

김 유 석

Anti-tumor Effects of the Tyrosine Kinase Inhibitor Rivoceranib in Canine Melanoma and Mammary Gland Tumor

By

You-Seok Kim

Advisor: Professor Hwa-Young Youn, DVM, PhD

A dissertation submitted to the faculty of the Graduate School of Seoul National University in partial fulfillment of the requirements for the degree of Doctor of Philosophy in Veterinary Clinical Science

February, 2020

DEPARTMENT OF VETERINARY CLINICAL SCIENCE

(MAJOR IN VETERINARY INTERNAL MEDICINE)

COLLEGE OF VETERINARY MEDICINE

GRADUATE SCHOOL OF SEOUL NATIONAL UNIVERSITY

개의 악성 흑색종 및 유선암에서 Tyrosine Kinase Inhibitor인 Rivoceranib의 항종양 효과

지도교수 윤 화 영

이 논문을 수의학 박사 학위논문으로 제출함

2019년 12월

서울대학교 대학원

수의학과 임상수의학 (수의내과학) 전공

김 유 석

김유석의 박사 학위 논문을 인준함

2020년 1월

위 원 장 김 민 수 (인)

부 위 원 장 윤 화 영 (인)

위 원 서 경 원 (인)

위 원 정 진 영 (인)

위 원 안 진 옥 (인)

Anti-tumor Effects of the Tyrosine Kinase Inhibitor Rivoceranib in Canine Melanoma and Mammary Gland Tumor

You-Seok Kim

(Supervised by Prof. Hwa-Young Youn, DVM, PhD)

Department of Veterinary Clinical Science
(Major in Veterinary Internal Medicine)
College of Veterinary Medicine
Graduate School of Seoul National University

Abstract

Cancer is one of the leading causes of death in dogs, and more than 50% of dogs over 10 years of age will develop at least one malignant tumor (London et al., 2003). In the United States, it has been reported that cancer is one of the leading causes of death in dogs over 2 years of age (Stephens et al., 2019).

As cancer occurs so frequently in dogs, often causing death, there is an urgent need for novel anti-tumor drugs for tumors that do not respond to the current standard therapies in human and veterinary medicine (Rutteman et al., 2013).

Tyrosine kinase is a protein that phosphorylates other proteins via their tyrosine residues and plays an important role in the normal cell signaling network which is closely involved in cell growth and differentiation. Vascular endothelial growth factor receptor (VEGFR) is expressed in vascular endothelial cells, and the VEGF-VEGFR interaction plays an important role in the migration and proliferation of endothelial cells (Thurston G et al., 2004). Platelet derived growth factor (PDGF) can promote angiogenesis, additionally PDGF as well as Platelet derived growth factor receptor (PDGFR) are expressed by the stroma and pericytes (London., 2009, Cherrington JM et al., 2000, McCarty MF et al., 2003).

Angiogenesis is considered a topic of major scientific interest in malignant tumor research. Recently, several angiogenic drugs, including anti-angiogenic

small molecule receptor tyrosine kinase inhibitors (TKIs), have demonstrated success in treating various carcinomas (Qin et al., 2019).

The studies mentioned above were conducted on tyrosine kinase abnormalities in human tumor research, but less research has been conducted in veterinary oncology (London., 2009).

Rivoceranib is a VEGFR2 inhibitor that targets microtubules in cancer cells thereby exerting antitumor effects, and has been reported to improve in human cancer patients. Thus, the aim of this study was to determine the anticancer effect of rivoceranib on canine melanoma cells (LMeC) and mammary tumor cells (CHMp) both *in vitro* and *in vivo*.

Cytotoxicity tests showed changes after 48h of drug treatment, at 6.25 and 12.5 μM in LMec and CHMp, respectively. In addition, cell growth decreased with increasing drug concentrations. Cell cycle analysis, cell apoptosis analysis, and western blot were conducted to investigate the mechanism of growth inhibition and cytotoxicity. As a result, the cytotoxic effects were primarily due to inhibition of cellular division through arrest of the G1 phase of the cancer cell lines, increased cell death and necrotic cells, and inhibition of VEGFR2 protein activity.

In addition, xenograft experiments were performed using a mouse tumor model implanted with LMeC and CHMp. Rivoceranib was administered orally

once a day at 75, 150 and 300 mg/kg for 28 days in LMeC xenograft models and for 15 days in CHMp xenograft models.

The LMeC xenograft model showed a significant decrease in tumor volume in the 150 mg/kg and 300 mg/kg treated groups compared to the vehicle control. The CHMp model showed significant decrease in tumor volume in all drug administered groups compared to the vehicle control. In addition, the weight of tumors extracted at necropsy were decreased with increasing drug concentrations.

The analysis of tumor tissues extracted at necropsy showed that Rivoceranib inhibited induction of apoptosis, inhibited cellular division and tumor vascularization.

This study is the first to look at the anticancer effect of Rivoceranib, a tyrosine kinase inhibitor, on canine melanoma and mammary gland tumors, and the results confirm the potential of Rivoceranib as an anticancer agent in canine tumor patients.

Keywords: dog / mammary gland tumor / melanoma / Rivoceranib / VEGFR2
Student number: 2016-36632

Contents

Mammary Gland Tumor in *in vitro* and *in vivo* Mouse Models

LIST OF FIGURES

LIST OF TABLES

ABBREVIATIONS

ALL	Acute lymphoblastic leukemia
ATP	Adenosine triphosphate
CC	Colorectal cancer
CHMp	Canine mammary gland tumor cells
CMGTs	Canine mammary gland tumors
CML	Chronic myelogenous leukemia
DTC	Differentiated thyroid cancer
EGFR	Epithelial growth factor receptor
FGFR	Fibroblast growth factor receptor
GIST	Gastrointestinal stromal tumor
LMeC	Canine melanoma cells
MCL	Mantle cell lymphoma
MDSCs	Myeloid derived suppressor cells
MTC	Medullary thyroid carcinoma
NHL	Non-Hodgkin's lymphoma
NSCLC	Non-small cell lung carcinoma
PDGF	Platelet derived growth factor
PDGFR	Platelet derived growth factor receptor
PlGF	Placental growth factor
RCC	Renal cell carcinoma

RTK	Receptor tyrosine kinase
TKI	Tyrosine kinase inhibitor
VEGF	Vascular endothelial growth factor
VEGFR	Vascular endothelial growth factor receptor

CHAPTER Ⅰ

Literature review

1. Tyrosine kinase inhibitors in the field of veterinary oncology

Cancer is one of the leading causes of death for dogs and is known to result in at least one malignant tumor in more than 50% of dogs over 10 years of age (London et al., 2003); in the United States, cancer has been reported as a leading cause of death in dogs over 2 years of age (Stephens et al., 2019).

The most common cancers in dogs are lymphomas, mast cell tumor (MCTs), sarcomas (fibrosarcoma, osteosarcoma, and hemangiosarcoma), carcinomas (mammary carcinoma, squamous cell carcinoma, and transitional cell carcinoma of the bladder) and malignant melanoma (Broodey RS., 1970, Cohen D et al., 1974). Most of these tumors occur over months to years and have microscopic metastasis at the time of diagnosis, which is similar in biological behavior to human cancers. The treatment of malignant tumors in dogs is therefore also similar to that in human cancer patients (London et al., 2003).

Tyrosine kinase is a protein that phosphorylates other proteins at the tyrosine residue and plays an important role in the cell signaling network system that is closely related to cell growth and differentiation (Paul et al., 2004).

Tyrosine kinases bind to adenosine triphosphate (ATP) and use it to add

phosphate groups to key tyrosine residues of themselves and other molecules, thereby creating intracellular signals that ultimately lead to gene transcription which affects cell proliferation and survival. This process usually begins in response to external signals produced by growth factors or other stimuli that initiate cascades of tyrosine phosphorylation. Protein kinases can be located on the cell surface, cytoplasm or nucleus (London et al., 2009).

Tyrosine kinases expressed on the cell surface often bind to growth factors that regulate their activation. They are usually present in the form of monomers on the cell surface, and binding to growth factors leads to dimerization and autophosphorylation, followed by initiation of kinase activity and phosphorylation of signaling intermediates (Madhusudan S et al., 2004, Zwick E et al., 2002). Examples of receptor tyrosine kinases are Kit, Met, Axl, and epithelial growth factor receptor (EGFR), all of which are known to have regulatory dysfunction in certain cancers (Fletcher JA et al., 2004, Laskin JJ et al., 2004, Ma PC et al., 2003, Neubauer A et al., 1997). In addition to regulating normal cellular function, certain tyrosine kinase receptors play an important role in promoting the growth of tumor blood vessels, also known as tumor angiogenesis. This includes vascular endothelial growth factor receptor (VEGFR), platelet derived growth factor receptor (PDGFR), fibroblast growth factor receptor (FGFR) and Tie1/2 (Cherrington JM et al., 2000, Eskens FA., 2003, London., 2009, McCarty MF et al., 2003, Thurston G et al., 2004).

VEGFR is expressed in vascular endothelial cells, and the VEGF-VEGFR interaction plays an important role in the migration and proliferation of endothelial cells (Thurston G et al., 2004). PDGF and PDGFR are expressed in

the stroma and pericytes, and PDGF can promote angiogenesis (Cherrington JM et al., 2000, London., 2009, McCarty MF et al., 2003).

Fibroblast growth factor synergistically interacts with VEGF to induce VEGF expression, thereby enhancing angiogenesis (Cherrington JM et al., 2000, London., 2009).

Angiogenesis is considered a topic of major scientific interest in malignant tumor research. Recently, several angiogenic target drugs, including anti-angiogenic small molecule receptor tyrosine kinase inhibitors (TKIs), have demonstrated success in treating various carcinomas (Qin et al., 2019).

Thus, many studies on tyrosine kinase abnormalities have been conducted in human tumor research, but less have been conducted in veterinary oncology (London., 2009).

Kit is a receptor found in mast cells and requires Kit signaling for differentiation, survival and function of mast cells (Ashman LK., 1999, Taylor ML et al., 2000, Zsebo KM et al., 1990)

Abnormal growth in solid cancers and hematologic malignancies involves complex interactions between neoplastic cells and the normal surrounding tissues (Hanahan D et al., 2000). Thus, tumor growth depends on factors derived from autocrine stimulation as well as the tumor microenvironment (paracrine stimulation). Tumor growth, progression and metastasis are mediated by the interaction of receptor tyrosine kinase (RTK) and downstream signaling molecules (Hanahan D et al., 2000). RTKs, through their regulation of various cellular processes and their role in cancer, especially in abnormal RTK signaling,

has caused them to be an relevant target for anticancer drug development (Schiffer CA., 2001, Traxler P et al., 2001).

The transition from cytotoxic chemotherapy to the discovery and development of molecularly-targeted cancer drugs has influenced the development of successful therapies which positively affect the lives of many cancer patients (Dervisis N et al., 2016). Imatinib, the BCR-ABL inhibitor, is considered one of the pioneering drugs that demonstrates effectiveness of designing small molecule therapeutics. Imatinib is a drug developed to treat patients with chronic myeloid leukemia caused by BCR-ABL translocation and has dramatically improved patient survival (Druker BJ et al., 2006). This success was followed by the development of other small molecule drugs that inhibit important cancer targets and changed the direction of modern anticancer drug development. In the field of human cancer research, nearly 20 kinase inhibitors have been approved by the FDA over the past four years (Dervisis N et al., 2016), (Table 1.1).

Veterinary oncology is slowly following the field of rapidly developing human oncology, with three FDA-approved kinase inhibitors and small molecular inhibitors at various stages of development (Dervisis N et al., 2016), (Table 1.2)., There are also a variety of TKIs that are used off-label as anticancer agents in dogs and cats (London et al., 2009), (Table 1.3).

2. Malignant melanoma and its treatment in veterinary medicine

Melanoma is a malignant tumor originating from melanocytes. Melanocytic neoplasms are known to occur in a variety of animal species, including humans, dogs, cats, horses, and wildlife and marine animals (Sweet et al., 2012).

Because dogs live so closely to humans, dogs are also affected by environmental factors thought to be associated with human chronic diseases and cancer (Nishiya et al., 2016).

Melanoma is one of the deadliest cancers, killing about 50, 000 people worldwide each year (Fowles et al., 2015, Haass et al., 2004). According to the American Cancer Society in 2015, approximately 73, 870 people (about 42, 670 men and 31, 200 women) were expected to be newly diagnosed with melanoma in 2015, and 9940 people (about 6640 men and 3300 women) were expected to die from the disease (Nishiya et al., 2016).

In veterinary medicine, the incidence of melanoma is about 3%, with 58 cases identified as melanocytic neoplasms out of 1313 tumors in a retrospective study of dogs (Kimura et al., 2012). In another retrospective study, 193 cases (8.9%) of the 2154 tumors diagnosed at the University of São Paulo between 2000 and 2006 were melanocytic neoplasms, including 186 cases (96.4%) in dogs and 7 cases (3.6%) in cats. It was found to be most prevalent in mixed-breed dogs of various ages with black hair coats (Teixeira et al., 2010).

Melanoma is the most common malignant tumor that occurs in the oral cavity and digits of dogs (Marino et al., 1995). Dermal melanoma is usually benign and can be treated with local resection, but oral melanoma and uveal melanoma progress rapidly and can metastasize to lung and surrounding lymph nodes as aggressive tumors.

Malignant melanomas are known not to respond well to conventional therapy at the time of diagnosis (Blackwood and Dobson, 1996; Quintin-Colonna et al., 1996; Todoroff et al., 1979). Classical clinical management includes: radical surgical excision (Clifford et al., 2013), radiation therapy, primary or adjuvant therapy, and combination therapy of chemotherapy and radiation therapy (Bergman et al., 2013). Controlling diseases with these classical therapies continues to present challenges (Almela et al., 2019).

It is increasingly known that the immune system plays an important role in the development and progression of cancer (La-Beck et al., 2015). In the treatment of cancer, chemotherapy and radiotherapy are mainly used to kill cancer cells. However, these methods have limitations such as systemic toxicities, bystander effects in normal cells, relapse of drug-resistant tumor cells, and inaction in micro metastases or subclinical disease states (Mellman et al., 2011). Moreover, there is no clear evidence of chemotherapy reducing metastasis as much as median survival time (MSTs), and local recurrence (Almela et al., 2019, Bergman et al., 2013). Therefore, research on more effective and tolerable immunotherapy based on immunological understanding of cancer are being actively conducted (Almela et al., 2019, Mellman et al., 2011)

Toceranib (Palladia®) is a drug that shows biological activity in canine

tumors such as mammary carcinoma, soft tissue sarcoma and anal gland adenocarcinoma (Mitchell L et al., 2012). In addition to cytotoxic effects in tumor cells, TKIs have been reported to have additional immunomodulatory effects on key immune cells recruited by tumors such as myeloid-derived suppressor cells (MDSCs) and regulatory T-lymphocytes (Treg). These cells play a central role in immune suppression, with the reversal of function being critical to the success of cancer immunotherapy (Mitchell L et al., 2012).

Rivoceranib is a novel tyrosine kinase inhibitor that is being developed in humans and is worth evaluation for treating melanoma in dogs.

3. Mammary gland tumor and its treatment in veterinary medicine

Breast cancer is the most commonly diagnosed cancer among women worldwide and is the leading cause of cancer-related deaths (Ghoncheh et al., 2016). In 2012, 2 million women worldwide were diagnosed with breast cancer (DeSantis et al., 2015), and the American Cancer Society estimated that 2350 cases in men and 231, 000 case in women were newly diagnosed in 2015 (Abdelmegeed et al., 2018). Consequently, prevention and therapeutic intervention of breast cancer are important aims for many researchers (Abdelmegeed et al., 2018).

Canine mammary gland tumors (CMGTs) are the most commonly diagnosed tumors in intact female dogs, with around 50% being malignant (Moe et al., 2001). Although the optimal treatment is unclear (Sorenmo et al., 2013), traditional surgery is still the main treatment for CMGT cases (De Campos et al., 2018).

However, about 50% of malignant tumors expressed as metastatic tumors will be identified as a relapse (Philibert et al., 2003, Simon et al., 2006). Adjuvant therapies may be required for high-risk, undifferentiated and advanced neoplasms (Novosad et al., 2003, Sorenmo et al., 2003), in addition, single-agent treatment is thought to be less effective than combination therapies. In solid cancers, angiogenesis has been reported to be clearly associated with disease progression

and metastasis (Raje et al., 2002). Therefore, it may be helpful to add anti-angiogenic treatment to conventional chemotherapy in the treatment of mammary gland tumors in dogs (DE Campos et al., 2018, Pierini et al., 2012).

Rivoceranib is a novel, small molecule anti-angiogenic drug, that is a selective VEGFR-2 tyrosine kinase inhibitor (Scott et al., 2018). In this study, we evaluated the effects of rivoceranib on canine mammary gland tumors.

4. Rivoceranib, tyrosine kinase inhibitor for cancer treatment

Rivoceranib, also known as apatinib, is a novel small molecule, which is a selective inhibitor of VEGFR-2 tyrosine kinase and is the second anti-angiogenic drug approved in China for advanced or metastatic gastric cancer treatment (Scott et al., 2018).

Angiogenesis is regulated by the interaction between tissue VEGFRs and their soluble ligands (VEGFs) and is maintained under finely regulated control under healthy conditions. VEGF molecules consist of various subvariants such as VEGF-A, VEGF-B, VEGF-C, VEGF-D and placental growth factor (PlGF). Similarly, the receptor family includes three molecular subtypes (VEGFR-1, VEGFR-2 and VEGFR-3), which are type-II transmembrane proteins characterized by tyrosine kinase (TK) activity (Ferrara et al., 2003, Roviello et al., 2016). The VEGF pathway, along with VEGFR-2, a key signaling receptor involved in this pathway, play a central role in angiogenesis (Karasic et al., 2017, Kowanetz et al., 2006, Pinto et al., 2017, Siemann et al., 2017). VEGFR-2 is abundantly expressed in endothelial cells and regulates the proliferation and migration pathways of these cells (Karasic et al., 2017, Kowanetz et al., 2006, Pinto et al., 2017, Siemann et al., 2017). Since physiological VEGF-mediated angiogenesis is rarely involved except in the female reproductive cycle and

wound healing, targeting VEGF is expected to have a relatively modest effect in physiological processes (Scott et al., 2018).

VEGFR-2 is thought to play a major role in tumor angiogenesis. Although this may eventually be associated with a worse clinical outcome, VEGFR-2 is currently an attractive target for novel anti-cancer therapies. Currently, various pharmacodynamics approaches such as receptor blockade (ramucirumab), blockade of the ligand (bevacizumab) and small-molecule inhibition (sorafenib, sunitinib, apatinib, cediranib, telatinib) can inhibit signals from VEGFR-2 activation (G. Roviello et al., 2016). Apatinib is now approved in China based on the results of the pivotal Chinese Phase III trial (Li et al., 2016) and is in orphan drug status as an advanced gastric cancer treatment in Europe, USA and Korea (Scott et al., 2018). Current ongoing Phase III trials will evaluate apatinib treatment in patients with advanced gastric adenocarcinoma (Scott et al., 2018).

In veterinary medicine, three kinase inhibitors have been approved by the FDA and several small molecular inhibitors are being developed at various stages (Dervisis N et al., 2016), (Table 1.2). Along with this trend, we will evaluate the potential of rivoceranib, a VEGFR-2 tyrosine kinase inhibitor, in dog tumors as a potential cancer treatment for dogs.

Table 1.1. Approved tyrosine kinase inhibitors in human medicine, 2011–2015

Drug	Target	Year Approved	Indication
Vandetanib (Caprelsa®)	Flt1, Flt4, KDR, EGFR, Ret	2011	MTC
Crizotinib (Xalkori®)	ALK, MET, EML4-ALK fusion protein	2011	NSCLC
Ruxolitinib (Jakafi®/Jakavi®)	JAK1, JAK2	2011	Myelofibrosis
Vemurafenib (Zelboraf®)	BRAF	2011	Melanoma
Bosutinib (Bosulif®)	BCR/ABL1	2012	CML
Axitinib (Inlyta®)	Flt1, Flt4, KDR, Kit, PDGF-R_/_	2012	RCC
Cabozantinib (Cometriq®)	KDR, Mek	2012	MTC
Regorafinib (Stivarga®)	KDR, TEK	2012	CC, GIST
Ponatinib (Iclusig®)	BCR/ABL1	2012	CML, ALL
Dabrafenib (Tafinlar®)	BRAF	2013	Melanoma
Trametinib (Mekinist®)	MEK1, MEK2	2013	Melanoma
Afatinib (Gilotrif®)	ERBB2, EGFR	2013	NSCLC
Ibrutinib (Imbruvica®)	BTK	2013	MCL, CLL
Tofacitinib (Xeljanz®)	JAK3	2013	Rheumatoid arthritis
Idelalisib (Zydelig®)	PI3-K	2014	CLL Follicular B-cell NHL
Ceritinib (Zykadia®)	ALK	2014	ALK+ NSCLC
Lenvatinib (Lenvima®)	VEGFR2 and VEGFR3	2015	Radioactive iodine-refractory DTC
Palbociclib (Ibrance®)	CDK4 and CDK6	2015	Breast carcinoma

ALL, acute lymphoblastic leukemia; CC, colorectal cancer; CML, chronic myelogenous leukemia; DTC, differentiated thyroid cancer; GIST, gastrointestinal stromal tumor; MCL, mantle cell lymphoma; MTC, medullary thyroid carcinoma; NHL, Non-Hodgkin's lymphoma; NSCLC, non-small-cell lung carcinoma; RCC, renal cell carcinoma.

Table 1.2. Approved tyrosine kinase inhibitors in veterinary medicine, all drugs

Drug	Target	Year Approved	Indication
Toceranib (Palladia®)	PDGF-R_ Kit Flt-3 RET JAK family	2009	Patnaik grade 2 or 3, recurrent, cutaneous mast cell tumors with or without regional lymph node involvement in dogs
Masitinib (Kinavet-CA1®)	Kit PDGF-R / Lyn FGF-R3	2010	Nonresectable grade 2 and 3 cutaneous mast cell tumors in dogs that have not previously received radiotherapy and/or chemotherapy except corticosteroids
Oclacitinib (Apoquel®)	JAK1, JAK2	2013	Control of pruritus associated with allergic dermatitis and control of atopic dermatitis in dogs at least 12 mos of age

Table 1.3. Tyrosine kinase inhibitors in veterinary oncology

Drug	Target	Tumor Types	Species	Dose
Toceranib (Palladia®)	PDGF-R_ Kit Flt-3 RET JAK family	sarcomas, carcinomas, melanoma, myeloma	Dogs	3.25 mg/kg EOD
Imatinib (Gleevec®)	Kit, Abl, PDGFR	MCTs, sarcomas	Dogs, cats	5 to 10 mg/kg SID

Chapter Ⅱ

Anti-tumor Effects of Rivoceranib Against Canine Melanoma in *in vitro* and *in vivo* Mouse Models

Abstract

Rivoceranib, a vascular endothelial growth factor receptor-2 (VEGFR2) inhibitor, exhibits anti-tumor effects by targeting the microtubules in cancer cells. Recently, the effects of rivoceranib on cancer have been improved in human patients. However, its effect against canine melanoma cells and the mechanisms underlying any such effect remain unclear. Herein, we investigated the anti-tumor effects of rivoceranib using *in vitro* and *in vivo* models. We performed cell proliferation, migration, and cell cycle analysis to determine the effects of rivoceranib on melanoma cells *in vitro*. Furthermore, apoptosis and angiogenesis in tumor tissues were examined by TUNEL assay and immunohistochemistry with an anti-CD31 antibody, respectively. Additionally, the expression levels of cyclin D1 and VEGFR2 activity were determined using western blot analysis. Rivoceranib treatment of canine melanoma cells had anti-proliferative effects and mediated cell cycle arrest. In animal experiments, after rivoceranib

administration, the average tumor volume and weight were significantly decreased compared to that with control treatment. Histologically, rivoceranib induced apoptosis and exerted anti-angiogenic effect in the tumor tissues. It also downregulated the expression of cyclin D1 and inhibited VEGFR2 activity. This is the first study to demonstrate the potential of rivoceranib as a therapeutic drug against canine melanoma.

Keywords: dog, melanoma, rivoceranib, LMeC, VEGFR2

2.1. Introduction

In animals, malignant melanoma occurs primarily in the nail bed and oral cavity (Stephan et al., 2013, Breit et al., 2014). Dermal melanoma is generally a benign disease that can be cured by local excision, but mucocutaneous, oral, and uveal melanoma are aggressive tumors that commonly metastasize to the regional lymph nodes and lungs, and malignant melanomas are poorly responsive to conventional therapies by the time they are discovered (Quintin-Colonna et al., 1996, Todoroff et al., 1979).

Angiogenic signals are novel anti-tumor targets that have been employed in therapeutic strategies against cancers. There is evidence that the inhibition of vascular endothelial growth factor receptor-2 (VEGFR2) can effectively suppress the proliferation, migration, and survivability of tumor cells (Huang et al., 2018). Currently, it is possible to inhibit the cell signal arising from the activation of VEGFR2 through several pharmacodynamic approaches, including receptor blockade (using ramucirumab), seizure of the ligand (using bevacizumab), and via the use of small-molecule inhibitors (using sorafenib, sunitinib, apatinib, cediranib, and telatinib) (Roviello et al., 2016).

Rivoceranib (also known as apatinib) is a novel, small molecule, selective VEGFR2 tyrosine kinase inhibitor and is an anti-angiogenic drug (Scott et al.,

2018). Previous studies have reported its improved therapeutic efficacy against various types of solid tumors (Hu et al., 2014, Langer et al., 2013, Li et al., 2013). However, it is not known whether rivoceranib would play a similar role in canine melanoma cells.

In this study, we aimed to investigate the anti-tumor effects of riv oceranib on canine melanoma cells using *in vitro* and *in vivo* models and tried to decipher the underlying mechanism by measuring the activity of VEGFR2. The results presented herein provide novel insights into the inhibition of VEGFR2 by rivoceranib in melanoma cells.

2.2 Materials and Methods

Cell culture

Melanoma cell line (LMeC) was provided by Professor Nobuo Sasaki (Inoue et al., 2004). LMeC cells were incubated in Roswell Park Memorial Institute (RPMI)-1640 medium, supplemented with 10% fetal bovine serum (FBS), 100 U/mL penicillin/streptomycin, at 37°C in a humidified atmosphere with 5% CO_2. The medium was replaced every 2–3 days, and the cells were sub-cultured at 90% confluency.

Cell proliferation assay

Rivoceranib powder was provided by HLB Life Science Co. Ltd. (Seongnam, Republic of Korea) and was stored at room temperature (20–25°C). To determine the concentration of rivoceranib that would have an effect on the proliferation and viability of LMeC cells, the powder was dissolved in dimethyl sulfoxide (DMSO; Duchefa Biochemie, Haarlem, the Netherlands) at a concentration of 40 mM. A total of 1,000 cells were plated in 96-well cell culture plates (SPL Life Science, Pocheon, Korea) with 100 μL culture medium containing different concentrations of rivoceranib (100, 50, 25, 12.5, 6.25, 3.125, and 0 μM). After 24, 48, and 72h of culture, 10 μL of D-Plus™ Cell Counting Kit (CCK)-8 dye solution (Dong-in Biotech, Seoul, Korea) was added to each well. After 1 h of incubation, the absorbance was detected at 450 nm using a spectrophotometer (US/680 Microplate reader, Bio-Rad). Wells containing the culture medium or 0.5% DMSO supplemented culture medium were used as the

control group.

Wound-healing assay

Migration of LMeC cells was determined using the wound-healing assay. The cells were seeded in a 12-well culture plate at a density of 1×10^5 cells/well. At 100% confluency, the cells were induced with 2 μg/mL of mitomycin (EnzoLife Science, Farmingdale, NY, USA) for 2 h. The bottom of the well was manually scratched with a sterile 1000 μL pipette tip and the dislodged cells were washed off with phosphate-buffered saline (PBS). The adherent cells were cultured in a medium with reduced serum concentration (2% FBS) to which rivoceranib was added at different concentrations (0, 12.5, and 25 μM). The migration of cells was captured under a microscope using the TCapture program (Tucsen Photonics, Fuzhou, China) at 0, 12 and 24h. The migration ability was calculated by determining the relative gap size with respect to that in the control group at 0h.

Cell cycle analysis

LMeC cells were cultured in 6-well cell culture plates. The cells were allowed to adhere to the surface and then cultured in the presence of rivoceranib (0, 12.5, and 25 μM). After 48h, the cells (1×10^5) were collected, washed with cold PBS, and fixed in 70% cold alcohol at -20°C for 2 h. The cells were again washed with PBS, and then incubated with 500 μL propidium iodide (PI)/RNase buffer (BD Biosciences, San Diego, CA, USA) for 30 min at room temperature. The samples were analyzed by flow cytometry (FACS, AriaII; BD Bioscience, San Jose, CA, USA).

Western blot analysis

Total protein from the collected LMeC cells and tumor tissue was extracted in PRO-PREP Protein Extraction Solution (Intron Biotechnology, Seongnam, Korea) on ice according to the manufacturer's instructions. Protein concentration was measured by Bio-Rad DC Protein Assay Kit (Bio-Rad, Hercules, CA, USA). The collected proteins (30μg) were separated by sodium dodecyl sulfate gel electrophoresis and the protein bands were transferred onto polyvinylidene difluoride membranes (EMD Millipore, Billerica, MA, USA). The membranes were incubated in 5% non-fat dry milk in Tris-buffered saline containing 0.1% Tween 20 for 1h and incubated with antibodies against anti-phospho-VEGFR2 (1:1000; Cell Signaling Technology, Beverly, Massachusetts, USA), Cyclin-D1 (1:1000; LSBio, Seattle, WA, USA) at 4℃ overnight. The membranes were incubated with anti-rabbit or anti-mouse IgG (Santa Cruz Biotechnology) as the secondary antibodies (1:2000) for 1 h. Immunoreactive bands were normalized to VEGFR2 (1:1000; Cell Signaling Technology) or β-actin (1:1000; Santa Cruz) and visualized by supersignal west pico PLUS Chemiluminescent substrate (Advansta, Menlo Park, CA, USA).

Apoptosis analysis

LMeC cells were seeded in 6-well cell culture plates at a density of 1×10^5 cells/well. After allowing the cells to adhere to the wells, they were treated with

different concentrations of rivoceranib (0, 12.5, and 25 μM) for 48h. Thereafter, the cells were harvested and washed with PBS. They were then stained with Annexin V and PI using the Annexin V Apoptosis Detection Kit I (BD Pharmingen, San Diego, CA, USA) according to the manufacturer's instructions. The apoptosis rate of LMeC cells was analyzed using FACS (BD Bioscience).

Mouse xenograft model

Female NOD.CB17-Prkdc^{SCID}/Acr mice aged 6 weeks and weighing 18–22 g were purchased from Raon Bio (Yonginsi, Korea). All the mice were housed in a specific pathogen-free standard room under controlled condition of temperature (~19–23°C), humidity (50% ± 20%), and light cycle (12-h light:12-h dark). The study and all the experimental procedures involving animals were approved by the Institutional Animal Care and Use Committee of KPC (P194007), and the experiments were performed as per the guidelines for animal experiments. To induce canine melanoma in mice, 1×10^7 cells were suspended in 100 μL PBS and mixed with 100 μL of Corning® Matrigel® Matrix (Corning Inc., New York, USA) (1:1 dilution). The cells were injected subcutaneously (SC) in the right flank. The tumor volume was determined using the following formula: $0.5 \times \text{width}^2 \times \text{length}$. The weight and tumor volume in mice were monitored every 3–4 days. Mice were euthanized when their body weights decreased by more than 15% or the tumor volume was more than 2500 mm^3 (10% of the body weight).

Rivoceranib treatment

For rivoceranib administration, the reagent powder was dissolved in 0.5%

carboxymethylcellulose (CMC) (Sigma–Aldrich, St. Louis, MO, USA) solution. Once the average tumor volume was 150–200 mm^3, the mice were randomized into four groups (n = 9, in each group): Group 1 mice were administered 10 mL/kg 0.5% CMC solution (vehicle); Group 2 mice were orally administered 10 mL/kg vehicle solution with 75 mg/kg rivoceranib; Group 3 mice were orally administered the vehicle solution with 150 mg/kg rivoceranib; Group 4 mice were orally administered the vehicle solution with 300 mg/kg rivoceranib. The rivoceranib and vehicle solutions were administered daily for 28 consecutive days. After 28 days, all the mice were sacrificed and their tumor tissues were collected for further analysis.

Immunofluorescence (IF) analysis

Xenograft tumor tissues obtained from mice were fixed in 10% formalin, and paraffin-embedded 4-μm-thick tissue sections were deparaffinized in xylene and rehydrated with ethanol. The tumor apoptosis rates were determined by TUNEL staining (Apo-BrdU DNA Fragmentation Assay Kit; BioVision, San Francisco, USA), following the manufacturer's instructions. For the analysis of angiogenesis ability in the tumor tissue, the slides were incubated overnight at 4 °C with antibodies against CD31 (1:100; Thermo Fisher Scientific, Waltham, MA, USA). After washing three times, the tumor sections were incubated with the secondary antibody (1:200; sc-516251; Santa Cruz Biotechnology) for 1 h at room temperature (protected from light). Finally, the slide was mounted in Vectashield mounting medium containing 4′,6-diamidino-2-phenylindole (Vector Laboratories, Burlingame, CA, USA). The immunoreactive cells were counted in six random

fields per group using an EVOS FL microscope (Life Technologies, Darmstadt, Germany).

Statistical analysis

Data are shown as means ± standard error. Differences between the groups were compared by one-way analysis of variance or Student's *t*-test using GraphPad Prism v.6.01 software (GraphPad Inc., La Jolla, CA, USA). A value of $P < 0.05$ was considered as statistically significant.

2.3 Results

Rivoceranib inhibits the proliferation and migration of LMeC cells *in vitro*.

To assess the effects of rivoceranib on the proliferation of LMeC cells, they were treated with different concentrations of the anti-cancer drug for 24, 48, and 72h. As revealed by the CCK-8 assay, rivoceranib displayed an inhibitory effect in a dose-dependent manner (figure 2.1A). The proliferation was significantly reduced at 25 μM after 24 ($p < 0.01$), 48($p < 0.01$) and 72h ($p < 0.01$) of treatment compared to that in the control group; the proliferation was also significantly reduced in the case of treatment with 6.25 μM rivoceranib after 48 ($p < 0.05$) and 72h ($p < 0.01$) compared to that in the control group. However, no significant reduction in the proliferation of cells was observed at 3.125 μM concentration. Therefore, for subsequent experiments, we treated the cells with 0, 12.5, and 25 μM of rivoceranib for 48h.

The effect of rivoceranib on the migration of LMeC cells was evaluated using the wound-healing assay. As shown in figure 1B, migration was significantly reduced in cells treated with rivoceranib in a concentration-dependent manner. These results confirmed the ability of rivoceranib to inhibit the mobility of LMeC cells *in vitro*.

Rivoceranib promotes cell cycle arrest in LMeC cells *in vitro*

The effect of rivoceranib on the cell-cycle progression of LMeC cells was investigated using FACS. The cells were treated with different concentrations (0, 12.5, and 25 μM) of rivoceranib for 48h. These cells were harvested and analyzed to determine their distribution among the G0/G1, S, and G2/M phases of the cell cycle. As shown in figure 2.2A, the G0/G1 ratio in the rivoceranib-treated groups was significantly higher compared to that in the untreated control group (0 μM) ($p < 0.01$), whereas the distribution of cells in the S and G2/M phases was significantly reduced in both the 12.5 ($p < 0.01$) and 25 μM ($p < 0.01$) treated groups compared to that in the untreated control group. To examine the expression levels of a cell cycle-related protein (cyclin D1), protein extracted from the collected LMeC cells was analyzed by western blotting. A comparison of relative band intensities confirmed that the expression of cyclin D1 was significantly lower in the rivoceranib-treated groups compared to that in the untreated control group ($p < 0.01$) and the difference between the 12.5 and 25 μM treated groups was also significant (figure 2.2B). These results suggest that rivoceranib induces G0/G1 cell cycle arrest through the downregulation of cyclin D1, thereby inhibiting the cell cycle progression in LMeC cells.

Rivoceranib induces apoptosis in LMeC cells and downregulates

the phosphorylation of VEGFR2 *in vitro*

To assess apoptosis, LMeC cells were treated with rivoceranib for 48h, and the harvested cells were subsequently analyzed by FACS after Annexin V/PI double staining. The percentage of apoptotic cells was significantly increased for LMeC cells treated with 12.5 ($p < 0.01$) and 25 μM ($p < 0.01$) of rivoceranib compared to that in the untreated control group (figure 2.3A). These results showed that rivoceranib also induces apoptosis in LMeC cells.

To investigate the potential mechanism of action of rivoceranib in LMeC cells, we examined the phosphorylation of VEGFR2 and determined the activity of VEGFR2 by western blot analysis. As shown in figure 2.3B, the relative band intensity was significantly lower in the treated groups than in the untreated control group, and there was no significant difference between the 12.5 ($p < 0.01$) and 25 μM ($p < 0.01$) treated groups. These results suggest that rivoceranib might be a promising anti-tumor drug for melanoma.

Rivoceranib suppresses tumor growth in a xenograft model

To further determine the anti-tumor activity of rivoceranib *in vivo*, we established an LMeC cell xenograft model by subcutaneous injection of LMeC cells suspended in Matrigel in mice. When the tumor volume was approximately 100–220 mm^3 at 21 days following inoculation, the mice were randomly divided

into four groups and were daily administered various concentrations of rivoceranib orally. The tumor volume in the control group (vehicle) was rapidly increased compared to that in the treated groups. After 29 days of treatment, the tumor growth curve showed that there was a significant reduction in the tumor volume in rivoceranib (150 and 300 mg/kg) (150mg/kg; $p < 0.01$, 300mg/kg; $p < 0.01$) treated groups compared to that in the control group (figure 2.4A, B). Furthermore, tumor weight was also measured after the mice were sacrificed; the results showed that tumor weight was significantly decreased in the mice treated with rivoceranib in a dose-dependent manner (figure 2.4C) (75mg/kg; $p < 0.05$, 150mg/kg; $p < 0.01$, 300mg/kg; $p < 0.01$). To evaluate the side effects of rivoceranib in mouse models, body weight was also measured. The body weight of mice in the treatment and control groups was similar, with no significant differences observed (figure 2.4D). The observations showed that rivoceranib also has anti-tumor effects in melanoma cell line xenograft mice; the results also suggest that rivoceranib treatment does not cause critical acute toxicity.

Rivoceranib induces apoptosis of cells and inhibits angiogenes is *in vivo*

Five tumor tissues per group that were selected randomly were sectioned and stained with TUNEL and anti-CD31 to evaluate the effect of rivoceranib on

cell apoptosis and angiogenesis, respectively. We found that rivoceranib treatment resulted in an increase in TUNEL-positive cells in a dose-dependent manner compared to that in the vehicle group as assessed in the blinded investigation (150mg/kg; $p < 0.01$, 300mg/kg; $p < 0.01$) (figure 2.5A, C). However, fewer CD31-positive cells were observed in the rivoceranib-treated tumor sections compared to that in the control (75mg/kg; $p < 0.01$, 150mg/kg; $p < 0.01$, 300mg/kg; $p < 0.01$) (figure 2.5B, C). Overall, these results indicated that rivoceranib also has apoptotic and anti-angiogenic effects *in vivo*.

Rivoceranib downregulates the phosphorylation of VEGFR2 a nd the expression of cyclin D1 *in vivo*

To further decipher the mechanism underlying the observed effects of rivoceranib, we checked the phosphorylation of VEGFR2 and the expression of cyclin D1 in 3 tumor tissues per group that were selected randomly. The results revealed that the expression of cyclin D1 (75mg/kg; $p < 0.01$, 150mg/kg; $p < 0.01$, 300mg/kg; $p < 0.01$) and VEGFR2 phosphorylation ratio (75mg/kg; $p < 0.05$, 150mg/kg; $p < 0.01$, 300mg/kg; $p < 0.01$) were significantly decreased in the rivoceranib-treated groups in a dose-dependent manner (figure 2.6). Together, the above results suggest that rivoceranib may inhibit the expression of cyclin D1 and downregulate the phosphorylation of VEGFR2 to induce the viability of

melanoma cells *in vivo*.

2.4 Discussion

Anti-angiogenic therapies have a wide application and they are not subject to resistance in clinical settings (Heath et al., 2009, Rapisarda et al., 2009). Rivoceranib is a highly selective VEGFR2 inhibitor and is the second-generation anti-angiogenic drug to be approved for the treatment of solid tumors in humans (Scott et al., 2018). However, its efficacy against canine melanoma cells has not been reported. In the present study, we confirmed the anti-tumor effects of rivoceranib using xenograft mouse models for canine melanoma.

Recent studies have reported that rivoceranib is effective against diverse types of tumors such as hepatocarcinoma, non-small cell lung cancer, and breast cancer (Gao et al., 2019, Liao et al., 2019, Zhang et al., 2019). In line with previous studies, our results indicate that the anti-tumor effects of rivoceranib can be attributed to the enhancement of apoptosis, inhibition of migration, and cell-cycle arrest in melanoma cells *in vitro* (Figure 2.1, 2.2, 2.3). We also demonstrate that the expression levels of cyclin D1, a cell cycle-related protein, were significantly reduced by rivoceranib treatment in a dose-dependent manner (Figure 2.2B). To further determine the anti-tumor activity of rivoceranib *in vivo*, we established an LMeC cell xenograft model. After oral administration of rivoceranib at doses of 0, 75, 150, and 300 mg/kg for 4 weeks in mice, the average

tumor volume and weight were significantly reduced in a dose-dependent manner (Figure 2.4A, B, C). In addition, the body weights of mice in the treatment and control groups were similar, and no significant differences were found (figure 2.4D).

Tumor angiogenesis is regulated by a variety of factors, and VEGF is one of the most important factors (Cao et al., 2019, Gao et al., 2019, Nishida et al., 2006). When tumor cells are stimulated by VEGF, VEGFR2 is autophosphorylated, resulting in the triggering of the downstream signaling pathways that promote angiogenesis (Ferrara et al., 2003, Holmes et al., 2007). It has been well established that VEGF/VEGFR2 signals promote the formation of neighboring vessels to facilitate the delivery of nutrients for the survival of cancer cells, and previous reports have shown that the expression of VEGFR2 correlated with a poor prognosis (Chen et al., 2017, Lian et al., 2019). Moreover, VEGF/VEGFR2 signals have beneficial effects on the survival of tumor cells (Ewald et al., 2014, Peng et al., 2016). Previous studies have shown that being an antagonist of VEGFR2, rivoceranib inhibits the VEGF-mediated viability and migration of tumor cells via the VEGFR2/RAF/MEK/ERK and PI3K/AKT pathways (Huang et al., 2018).

We also showed that rivoceranib significantly reduces the activity of VEGFR2 *in vitro* and *in vivo* using western blot analysis (Figure 2.3B and 2.6).

Furthermore, tumor sections were subjected to TUNEL staining and were probed with the anti-CD31 antibody to evaluate the effect of rivoceranib on the apoptosis and angiogenesis of the cells. We found that rivoceranib treatment resulted in increased TUNEL-positive cells compared to that in the vehicle group (Figure 2.5A), whereas, fewer CD31-positive cells were observed in the rivoceranib-treated tumor sections (Figure 2.5B).

Based on the above results, we hypothesize that rivoceranib reduces the viability and tumor angiogenesis in canine melanoma cells via the inhibition of VEGF/VEGFR2. However, whether rivoceranib could perform the same anti-tumor function in melanoma canine patients still needs to be studied further.

In conclusion, our results suggest that rivoceranib inhibits the proliferation, migration, and cell-cycle progression in melanoma cells. In animal experiments also, rivoceranib showed therapeutic efficacy in xenograft mouse models through enhancement of apoptosis and anti-angiogenic effect via VEGFR2 signaling. These results suggest that rivoceranib may be a novel anti-angiogenic therapy in canine melanoma.

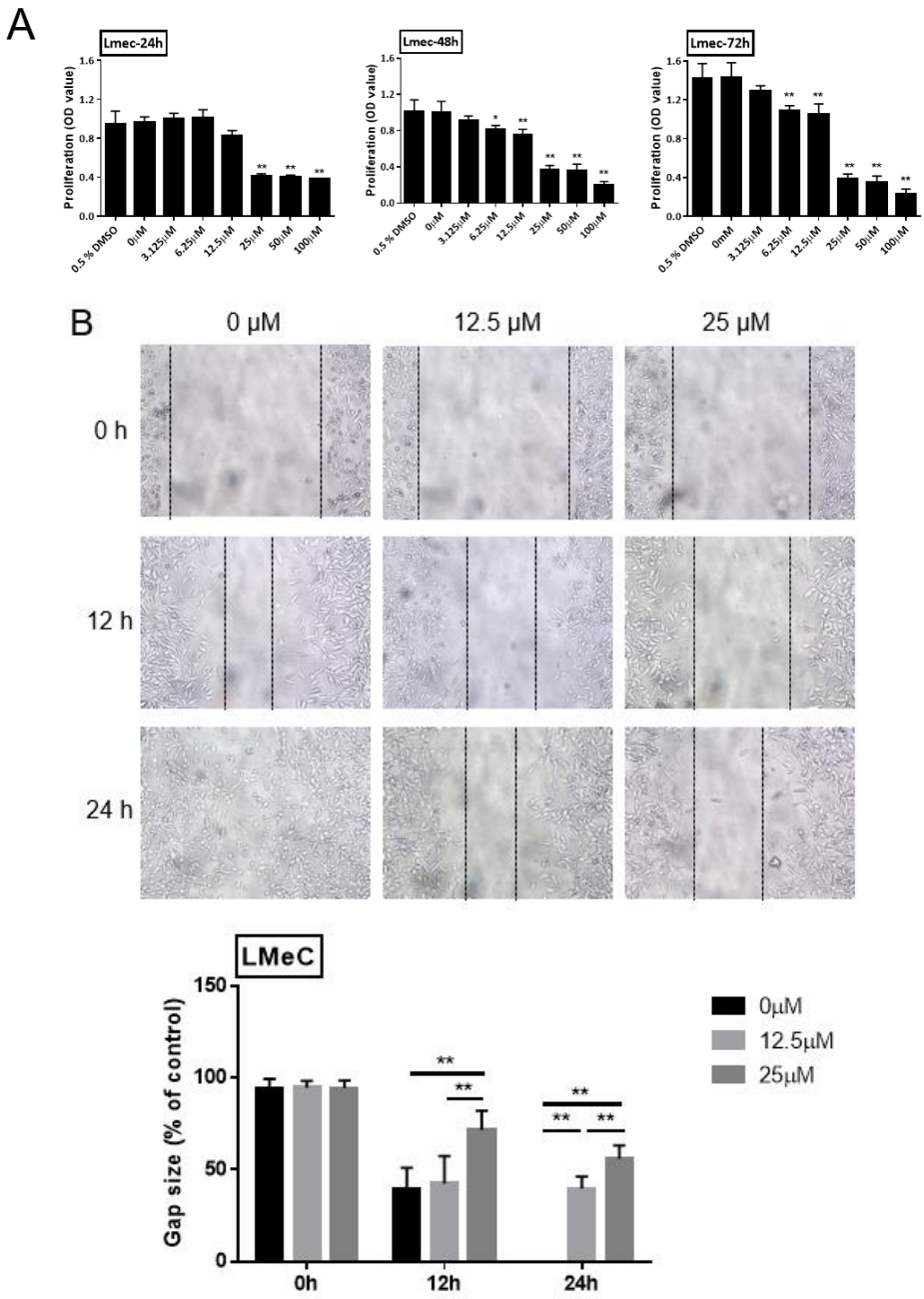

Figure 2.1. Effects of rivoceranib on the proliferation and migration of cells *in vitro*. (A) Viability of LMeC cells after treatment with different concentrations

of rivoceranib at 24, 48, and 72h of treatment. (B) Cell migration capacity of LMeC cells at 24, 48, and 72h of rivoceranib treatment. All the experiments were performed in triplicates. The data represent means ± standard deviation obtained from three independent experiments. * $p < 0.05$, ** $p < 0.01$ versus the control group (0.5% dimethyl sulfoxide) at the same time point.

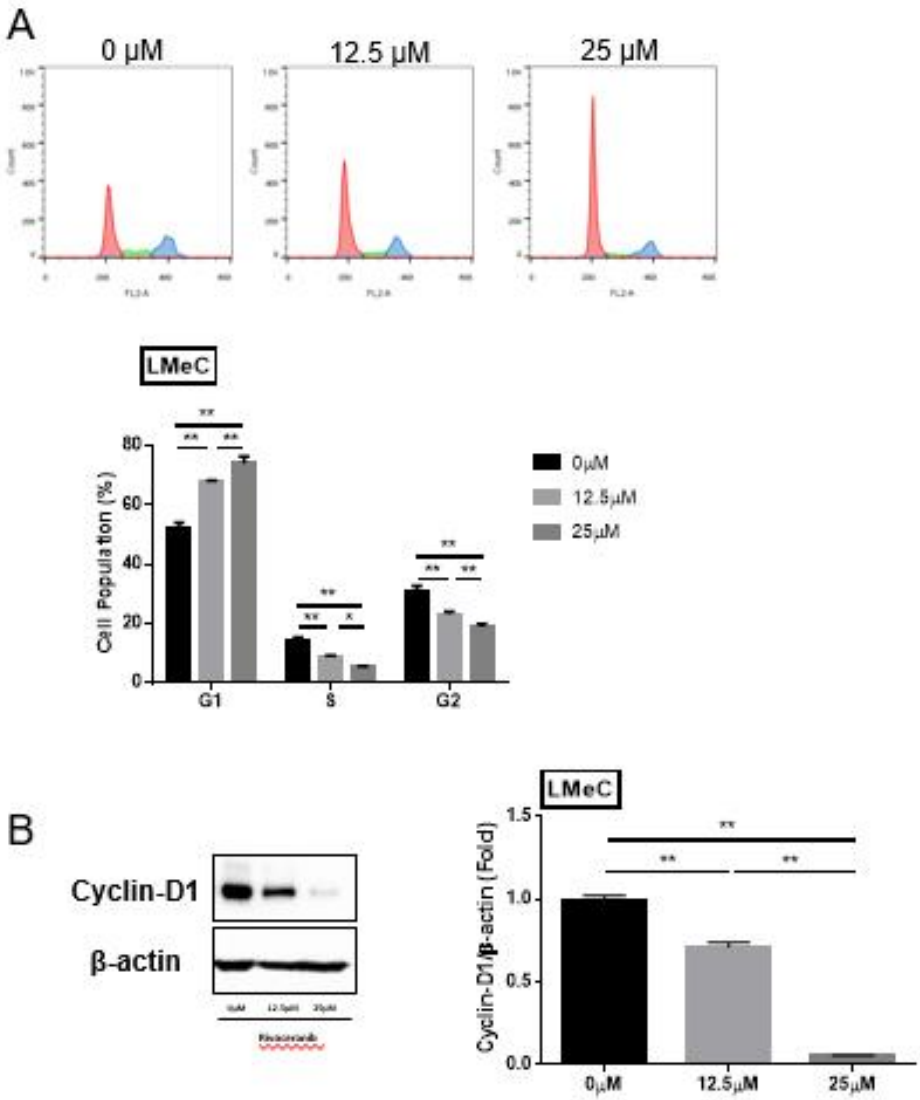

Figure 2.2. Effects of rivoceranib on cell cycle arrest *in vitro*. (A) Cell-cycle distribution of LMeC cells treated with rivoceranib was analyzed by flow cytometry at 48h. (B) The expression levels of cyclin D1 were measured using western blot analysis. The intensity of the band on films is presented as the relative ratio of cyclin D1 to the band intensity of β-actin. The data represent

means ± standard deviation obtained from three independent experiments. * $p < 0.05$, ** $p < 0.01$.

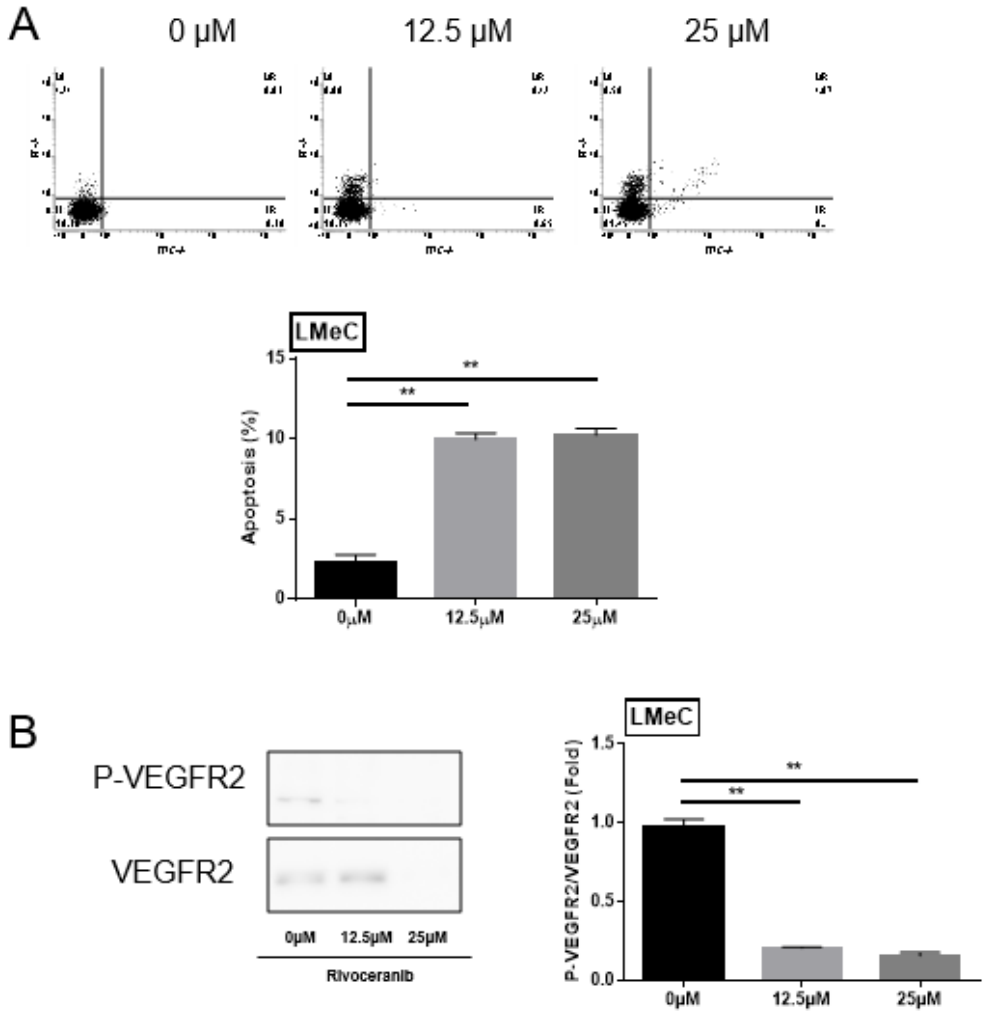

Figure 2.3. Effects of rivoceranib on the apoptosis of LMeC cells and on VEGFR2 phosphorylation *in vitro*. (A) The percentage of apoptotic cells was measured by flow cytometry. Apoptotic cells were quantified using Annexin V (FITC) and propidium iodide (PI) double staining. (B) The activity of VEGFR2 was analyzed by determining the VEGFR2 phosphorylation ratio using western blot analysis. The intensity of the band on the films is presented as the relative

ratio of p-VEGFR2 to the band intensity of VEGFR2. The data represent means ± standard deviation obtained from three independent experiments. ** $p < 0.01$.

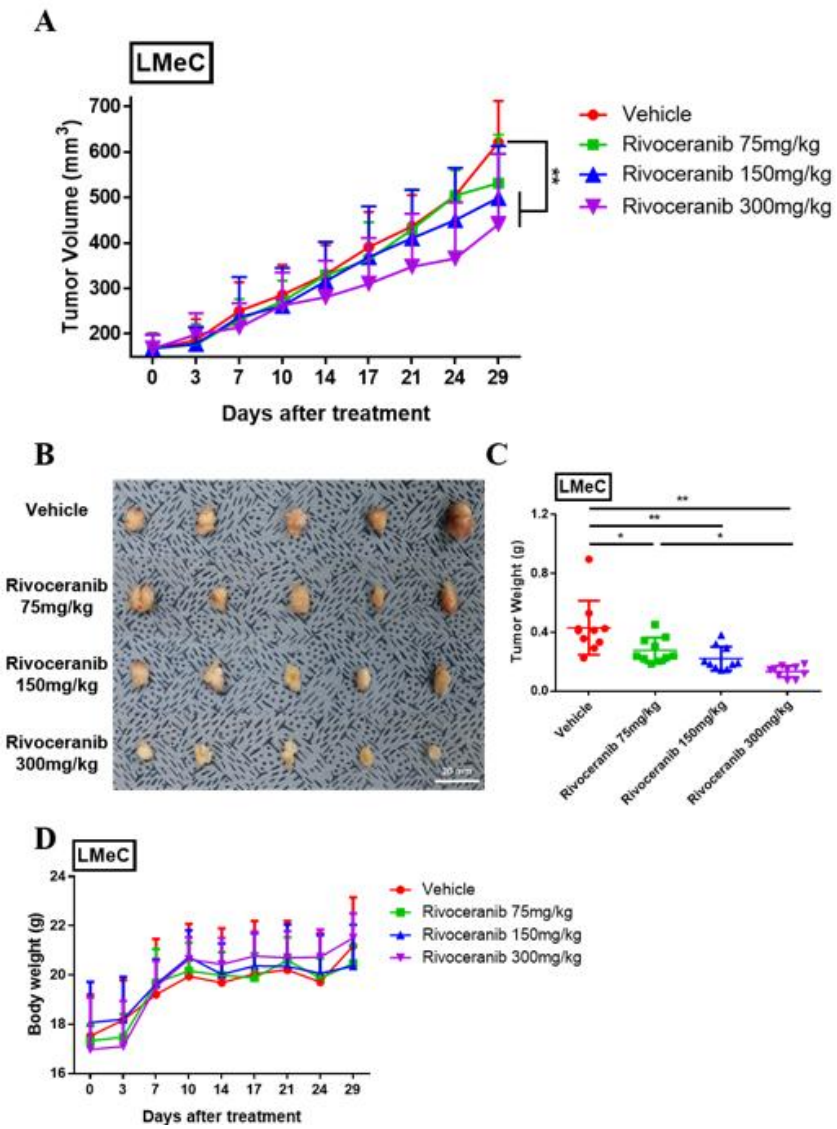

Figure 2.4. *In vivo* effects of rivoceranib in xenograft model. (A) The mean tumor volumes in the four groups (vehicle, 75 mg/kg, 150 mg/kg, and 300 mg/kg rivoceranib-treated). (B) Representative images of the collected tumors from the xenograft models after 29 days of treatment, and (C) tumor weight. (D) The body

weights of mice were monitored twice a week during the rivoceranib treatment. The data represent means ± standard deviation * $p < 0.05$, ** $p < 0.01$.

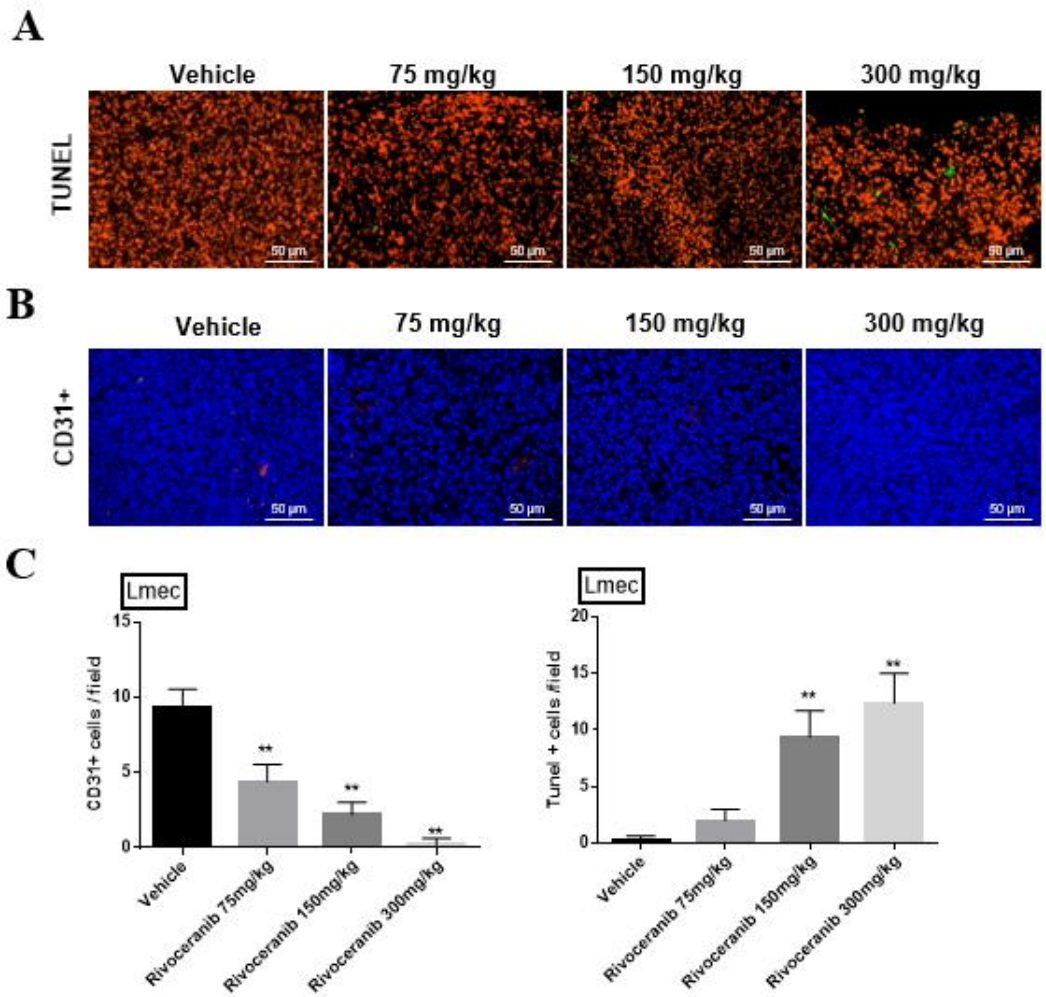

Figure 2.5. Effects of rivoceranib on apoptosis and angiogenesis *in vivo*. (A, B) TUNEL and anti-CD31 staining images of tumor sections in each group (vehicle, 75 mg/kg, 150 mg/kg, and 300 mg/kg). (C) TUNEL- and CD31-positive cells were counted in six random fields per group under a microscope (200× magnification). The data represent means ± standard deviation. ** $p < 0.01$ versus control group (vehicle group).

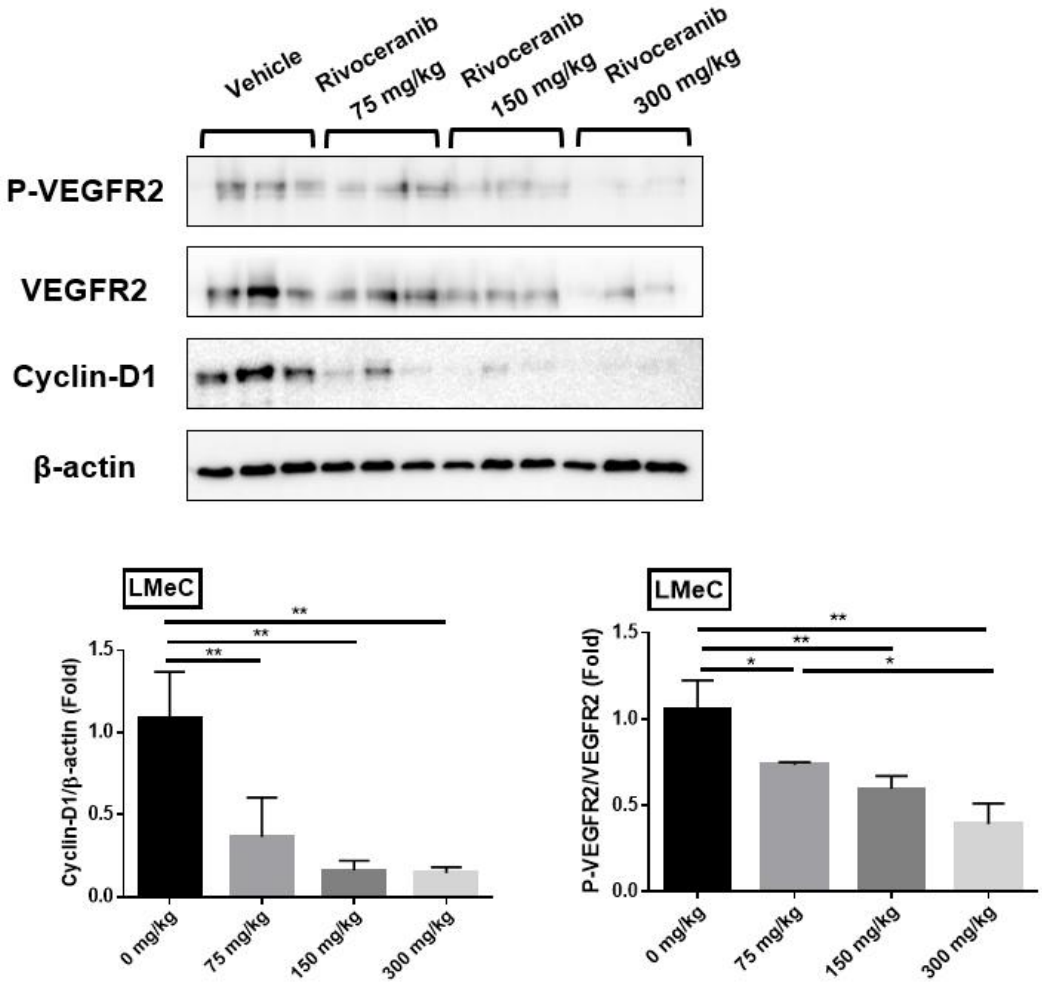

Figure 2.6. Effects of rivoceranib on the protein levels of phosphorylated VEGFR2 and cyclin D1. The collected tumor tissues were subjected to western blot analysis for the evaluation of VEGFR2 activity and the expression level of cyclin D1. The intensity of band on films is presented as the relative ratio of p-VEGFR2 to the band intensity of VEGFR2, and ratio of cyclin-D1 to the band intensity of β-actin. The data represent means ± standard deviation obtained from three independent experiments. * $p < 0.05$, ** $p < 0.01$.

Chapter Ⅲ

Anti-tumor Effects of Rivoceranib Against Canine Mammary Gland Tumor in *in vitro* and *in vivo* Mouse Models

Abstract

Rivoceranib, a vascular endothelial growth factor receptor 2 (VEGFR2) inhibitor, exhibits antitumor effects by targeting the microtubules of cancer cells. Recently, the effects of rivoceranib on canine mammary gland tumors (MGTs) have been reported, but its mechanism of action is unclear. Hence, we first examined the efficacy of rivoceranib on canine MGTs *in vitro* by analyzing its effects on cell proliferation, migration, cycle, and apoptosis Furthermore, the *in vivo* antitumor activity was evaluated using a CHMp cell xenograft model. Rivoceranib treatment of canine MGTs induced antiproliferative effects and cell cycle arrest *in vitro*. In animal experiments, rivoceranib deceased the average volume of mammary gland tumors to approximately 70% of the untreated control tumors. Histologically, rivoceranib showed antiangiogenic effects and induced apoptosis of tumor cells. In addition, rivoceranib downregulated the expression levels of cyclin D1 and VEGFR2 activity *in vitro* and *in vivo*. These

results support the potential application of rivoceranib as a novel chemotherapeutic strategy for canine MGTs and melanoma.

Keywords: dog, mammary gland tumor, Rivoceranib, CHMp, VEGFR2

3.1. Introduction

Canine mammary gland tumors (MGTs) are the most frequently diagnosed tumors in intact female dogs and 50% are malignant (Moe et al., 2001). Although the optimal extent of conventional surgery remains unclear (Sorenmo et al., 2013), it is still the main treatment for canine MGTs. However, approximately 50% of malignant tumors exhibiting metastasis will probably recur (Philibert et al., 2003, Simon et al., 2006). Adjuvant therapies may be required for high-risk, undifferentiated, and advanced neoplasms (Novosad et al., 2003, Sorenmo et al., 2003).

Angiogenesis has been identified to have a crucial role in solid tumor malignancy, and is essential in the process of tumor proliferation, survival, and metastasis (Hanahan et al., 2000, 2011, Kerbel et al., 2006). The vascular endothelial growth factor (VEGF) family and its receptors (VEGFRs) are considered the core signaling pathway in tumor angiogenesis-related molecular mechanisms (Zhang et al., 2019). Several previous studies have demonstrated that VEGFR2 plays an important role in angiogenesis of MGTs (Banerjee et al., 2007, Gao et al., 2019, Li et al., 2010).

Recently, various anti-angiogenic drugs such as rivoceranib (apatinib), sorafenib, sunitinib, cediranib, and telatinib have been evaluated in human clinical studies (Kang et al., 2014, Moehler et al., 2011, Roviello et al., 2016, Qin et al.,

2014). Rivoceranib, a novel oral small-molecule tyrosine kinase inhibitor of VEGFR-2, blocks endothelial and tumor cell proliferation and migration, thus, inhibiting tumor growth (Scott et al., 2018, Yu et al., 2019).

Presently, the effects of rivoceranib have been demonstrated in canine MGTs in an *in vivo* study (Lee et al., 2019); however, the mechanism of action is unclear. Hence, we examined the antitumor effects of rivoceranib on canine MGTs *in vitro* and *in vivo*. Moreover, we explored the potential mechanism of the inhibitory effects of rivoceranib on canine MGTs to provide a potential new strategy for the treatment of canine patients.

3.2 Materials and Methods

Cell culture

Mammary gland tumor Cell line (CHMp) were obtained from the Department of Veterinary Pharmacology, Seoul National University. CHMp cells were incubated in the Roswell Park Memorial Institute (RPMI)-1640 medium, supplemented with 10% fetal bovine serum (FBS), 100U/ml penicillin/streptomycin, at 37°C in a humidified atmosphere with 5% CO_2. The media were replaced every 2-3 days, and the cells were sub-cultured upon reaching 90% confluency.

Cell proliferation assay

Rivoceranib powder was provided by HLB Life Science Co., Ltd. (Seongnam, Republic of Korea) and store at room temperature (20–25℃). To determine the concentration of rivoceranib that affects CHMp cell viability and proliferation, 1,000 of cells were plated onto 96-well cell culture plates (SPL Life Science, Pocheon, Korea) with 100 μL culture medium containing rivoceranib (100, 50, 25, 12.5, 6.25, 3.125, or 0 μM). After culturing for 24, 48, and 72h, the cell number was measured using the D-plus^{tm} cell counting kit (CCK)-8 (Dong-in Biotech, Seoul, Korea) assay, following the manufacturer's instructions. Wells containing culture medium or 0.5% dimethyl sulfoxide (DMSO) with culture medium were used as the control group.

Wound-healing assay

The migration of CHMp cells was determined using a wound-healing assay. The cells were seeded in 12-well culture plate at a density of 1×10^5 cells/well. After reaching 100% confluence, the cells were induced using 2 μg/mL mitomycin (EnzoLife Science, Farmingdale, NY, USA) for 2 h. CHMp cells were manually scratched using a sterile 1000 μL pipette tip and suspended cells were removed with phosphate-buffered saline (PBS). The various groups of adherent cells were cultured in serum-reduced complete medium (2% FBS) with rivoceranib (0, 12.5, and 25 μM). The cell migration was observed and captured under a microscope using the TCapture program (Tucsen Photonics, Fuzhou, China) at 0, 12, and 24h. The migration ability was calculated relative to the gap size of the control group at 0h.

Cell cycle assay

CHMp cells were cultured in six-well cell culture plates, allowed to adhere, and then they were further cultured with increasing concentrations of rivoceranib (0, 12.5, and 25 μM). After 48h, 1×10^5 cells were collected, washed with cold phosphate-buffered saline (PBS), and fixed with 70% cold alcohol at -20°C for 2 h. Then the cells were collected, washed again with PBS, and incubated with 500 μL propidium iodide (PI)/RNase buffer (BD Biosciences, San Diego, CA, USA) for 30 min at room temperature. The samples were analyzed using flow cytometry (fluorescence-activated cell sorting [FACS], AriaII flow cytometer; BD Bioscience, San Jose, CA, USA).

Western blot analysis

Total protein from the collected CHMp cells and tissue was extracted in PRO-PREP Protein Extraction Solution (Intron Biotechnology, Seongnam, Korea) on ice according to the manufacturer's instructions. Concentration of protein was measured using Bio-Rad DC Protein Assay Kit (Bio-Rad, Hercules, CA, USA). The collected proteins (30μg) were separated by sodium dodecyl sulfate gel electrophoresis and the protein bands were transferred onto polyvinylidene difluoride membranes (EMD Millipore, Billerica, MA, USA). The membranes were incubated in 5% non-fat dry milk in Tris-buffered saline containing 0.1% Tween 20 for 1h and incubated with antibodies against anti- Cyclin-D1 (1:1000; LSBio, Seattle, WA, USA) and anti-phospho-VEGFR2 (1:1000; Cell Signaling Technology, Beverly, Massachusetts, USA), at 4℃ overnight. The membranes were incubated with anti-mouse IgG or anti-rabbit (Santa Cruz Biotechnology) as the secondary antibodies (1:2000) for 1 h. Immunoreactive bands were normalized to β-actin (1:1000; Santa Cruz) or VEGFR2 (1:1000; Cell Signaling Technology) and visualized using supersignal west pico PLUS Chemiluminescent substrate (Advansta, Menlo Park, CA, USA).

Apoptosis analysis

CHMp cells were seeded in six-well cell culture plates at a density of 1×10^5 cells, allowed to adhere, and then they were treated with different concentration of rivoceranib (0, 12.5, and 25 μM) for 48h. The cells were then dual stained with annexin V and PI using the Annexin V apoptosis detection kit I (BD Pharmingen, San Diego, CA, USA) according to the manufacturer's

instructions. The apoptosis rate of CHMp cells was analyzed using a FACS cytometer (BD Bioscience).

Mouse xenograft model

Female NOD.CB17-Prkdc^{SCID}/Acr mice aged 6 weeks and weighing 18–22 g were purchased from Raon Bio (Yonginsi, Korea). All mice were housed in a specific pathogen-free standard room under controlled temperature (19–23℃) and humidity (50 ± 20%) conditions and a 12-h light-dark cycle. The study and all experimental procedures involving animals were approved by Institutional Animal Care and Use Committee of KPC (P194007), and the experiments were performed in adherence to the guidelines for animal experiments. To induce tumors in the mice, 5 × 10^6 CHMp cells were suspended in 100 μL PBS, mixed with 100 μL Corning® Matrigel® Matrix (1:1 dilution, Corning Inc., New York, NY, USA), and then injected subcutaneously (SC) into the right flank of each mouse. After the predetermined inoculation and treatment periods, tumor dimensions were measured and the volume was calculated using the following formula: 0.5 × width^2 × length. The weight and tumor volume of the mice were monitored every 3–4 days. Mice were euthanized when their body weight reduced by > 15 % or the tumor volume was > 2500 mm^3.

Rivoceranib treatment

For rivoceranib administration, the reagent powder was dissolved in 0.5% carboxymethylcellulose (CMC, Sigma-Aldrich, St. Louis, MO, USA) solution. When the tumors reached an average volume of 150–200 mm^3, the mice were

randomized into the following four groups (n = 9 each) and were orally treated as indicated: Group 1, 10 mL/kg 0.5% CMC solution (vehicle); and Groups 2, 3, and 4 were administered 75, 150, and 300 mg/kg rivoceranib, respectively in 10 mL/kg of the vehicle. Rivoceranib and the vehicle were administered daily for 16 consecutive days and then all mice were euthanized and tumor tissue samples were collected for further analysis.

Immunofluorescense (IF) analysis

Xenograft tumor tissues from the mice were fixed in 10% formalin, paraffin-embedded, and then 4 μm-thick tissue sections were cut, mounted on slides, followed by deparaffinization in xylene and rehydrated with an ethanol solution. The tumor apoptosis rates were determined using the terminal deoxynucleotidyl transferase (TdT) deoxyuridine dUTP nick-end labeling (TUNEL) assay (Apo-BrdU DNA fragmentation assay kit; BioVision, San Francisco, CA, USA), following the manufacturer's instructions. For analysis of tumor tissue angiogenesis, slides were incubated overnight at 4℃ with antibodies against CD31 (1:100; Thermo Fisher Scientific, Waltham, MA, US). After washing three times, the tumor sections were incubated with the secondary antibody (1:200, sc-516251, Santa Cruz Biotechnology) for 1 h at room temperature (protected from light). Finally, the slides were mounted in a Vectashield mounting medium containing 4′,6-diamidino-2-phenylindole (Vector Laboratories, Burlingame, CA, USA) and immunoreactive cells were counted in six random fields per group using an EVOS FL microscope (Life Technologies, Darmstadt, Germany).

Statistical Analysis

Data are shown as mean ± standard error. Differences between groups were compared by one-way analysis of variance or Student's t test with GraphPad Prism v.6.01 software (GraphPad Inc., La Jolla, CA, USA). $P < 0.05$ was considered as statistically significant.

3.3 Results

Rivoceranib inhibited the proliferation and migration of CHMp cells *in vitro*.

The assessment of the effects of different concentrations of rivoceranib on CHMp cell proliferation following treatment for 24, 48, and 72h showed a dose-dependent inhibition (figure 3.1). Cell proliferation was more significantly reduced by treatment with rivoceranib 25 μM at all time points and 2.5 μM after 48h than it was by the control (vehicle) treatment. However, no significant reduction in proliferation of CHMp cell was observed at concentrations < 6.25 μM. The CCK assay showed that rivoceranib treatment significantly inhibited CHMp cell proliferation and in further assays, cells were treated 0, 12.5, and 25 μM rivoceranib for 48h.

Evaluation of the effect of rivoceranib on CHMp cell migration using a wound-healing assay showed a significant concentration dependent reduction in cells treated with rivoceranib (figure 3.1B). These results confirmed the ability of rivoceranib to inhibit the mobility of CHMp cells *in vitro*.

Rivoceranib promoted cell cycle arrest of CHMp cells *in vitro*

The FACS analysis of the effect of rivoceranib on cell cycle progression of CHMp cells incubated with different concentrations (0, 12.5, and 25 μM) of

rivoceranib for 48h, determined their distribution in G0/G1, S, and G2/M cell cycle phases. Figure 3.2 shows that the G0/G1 phase ratios of the rivoceranib-treated groups (12.5 and 25 μM) were significantly increased compare with that of the vehicle treated control group (0 μM) ($p < 0.01$), while the G2/M distribution was significantly reduced in both the 12.5 ($p < 0.05$) and 25 μM ($p < 0.01$) treated groups compared that of the control group.

In contrast, the S phase distribution was similar between the rivoceranib-treated and untreated control groups. The expression of the cell cycle related protein (cyclin D1) was analyzed in CHMp cells using western blotting. The relative band density confirmed that cyclin D1 expression was significantly lower in the rivoceranib treatment groups than it was in the untreated conrol group, and the difference between the 12.5 and 25 μM treated groups was also significant (figure 3.2). The results suggest that rivoceranib induced G0/G1 cell cycle arrest by downregulating cyclin D1 expression, thereby inhibiting cell cycle progression of CHMp cells.

Rivoceranib induced apoptosis of CHMp cells and downregulated VEGFR2 phosphorylation *in vitro*

The assessment of the apoptosis rate of CHMp cells using FACS with Annexin V/ PI double staining showed a more significant increase following

treatment with 12.5 and 25 μM rivoceranib for 48h than with the vehicle (control, figure 3.3). The results indicated that rivoceranib induced apoptosis of CHMp cells.

To investigate the potential mechanism of action of rivoceranib in CHMp cells we next examined VEGFR2 phosphorylation to determine its activity using western blotting. Figure 3.3B shows that the relative band density was significantly lower in the treatment groups than in the untreated control group, and there is no significant difference between the 12.5 and 25 μM treated groups. The results suggested that rivoceranib may be a promising anticancer drug against mammary gland tumors.

Rivoceranib suppressed tumor growth in xenograft model

To further determine the antitumor activity of rivoceranib *in vivo*, we established an CHMp cell xenograft model by subcutaneous injection of CHMp cells suspended in Matrigel in mice. When the tumor volume was approximately 10–240 mm^3 at 9 days following inoculation, the mice were randomly divided into four groups and were daily administered various concentrations of rivoceranib orally. The tumor volume of the control group (vehicle) increased more rapidly than that of the treated groups did. After 16 days of treatment, the tumor growth curve showed that there was a significant reduction in the tumor volume in all

rivoceranib (75, 150 and 300 mg/kg) (75mg/kg; $p < 0.01$, 150mg/kg; $p < 0.01$, 300mg/kg; $p < 0.01$) treated groups compared to that in the control group (figure 3.4A, B). Furthermore, tumor weight measurement after the mice were sacrificed showed a significant dose dependent decrease in 150mg/kg and 300mg/kg rivoceranib treated mice (figure 3.4C) (150mg/kg; $p < 0.01$, 300mg/kg; $p < 0.01$). To evaluate the side effects of rivoceranib on the mouse model, body weight also measured during this study and values of the treatment and control groups were similar with no significant differences (figure 3.4D). These observations indicted that rivoceranib showed antitumor effects on CHMp cell xenografted mice, with no acute toxicity response following treatment.

Rivoceranib induced cell apoptosis and inhibited angiogenesis *in vivo*

Five tumor tissues per group that were selected randomly were sectioned and stained with TUNEL and anti-CD31 to evaluate the effect of rivoceranib on cell apoptosis and angiogenesis, respectively. We found that the rivoceranib-treatment increased TUNEL-positive cells more than the vehicle treatment did, in dose-dependent manner (150mg/kg; $p < 0.01$, 300mg/kg; $p < 0.01$) (figure 3.5A, C). However, fewer CD31-positive cells were observed in the rivoceranib-treated tumor sections compared to that in the control (75mg/kg; $p < 0.01$, 150mg/kg; $p <$

0.01, 300mg/kg; $p < 0.01$) (figure 3.5B, C). Overall, these results indicated that rivoceranib showed apoptotic and anti-angiogenic activity *in vivo*.

Rivoceranib downregulated VEGFR2 phosphorylation and cyclin D1 expression *in vivo*

To further reveal the underlying mechanism of action of rivoceranib, we investigated its effects on VEGFR2 phosphorylation and cyclin D1 expression in 3 tumor tissues per group that were selected randomly. The results revealed that the expression of cyclin D1 (75mg/kg; $p < 0.01$, 150mg/kg; $p < 0.01$, 300mg/kg; $p < 0.01$) and VEGFR2 phosphorylation ratio (75mg/kg; $p < 0.05$, 150mg/kg; $p < 0.01$, 300mg/kg; $p < 0.01$) were significantly decreased in the rivoceranib-treated groups in a dose-dependent manner (figure 3.6). These results suggest that rivoceranib likely inhibited cyclin D1 and downregulated VEGFR2 phosphorylation to reduce mammary gland tumor cell viability *in vivo*.

3.4 Discussion

The aggressiveness of CMGTs has made this disease one of the leading causes of death in female dogs (Igase et al., 2016). Although the antitumor effects of rivoceranib on canine MGTs have been proven in a previous study (Lee et al., 2019), its mechanism of action remains unclear. Thus, we confirmed the antitumor effects of rivoceranib and further investigated its potential underlying mechanisms using a xenograft mouse model of canine melanoma.

In line with our previous study, the present results indicated that the antitumor effects of rivoceranib were attributable to enhanced cell apoptosis, anti-migration, and cell cycle arrest *in vitro*. We also demonstrated that expression levels of cyclin D1, a G0/G1 phase-related protein, were significantly reduced by rivoceranib treatment in a dose-dependent manner. The established CHMp cell xenograft mouse model was a suitable experimental model, which aided in the successful determination of dose-dependent effects of rivoceranib. Moreover, the comparable body weights of mice after rivoceranib and vehicle treatment with no significant differences indicated the promising low toxicity of rivoceranib.

VEGFR2 exerts its biological function by coupling with VEGF cytokines to activate the VEGF/VEGFR2 signaling pathway, which is closely related to tumor angiogenesis and has a crucial role in tumor cell adaptation to hostile environments (Gao et al., 2019, Nishida et al., 2006). VEGF/VEGFR2 has been

well-established to promote neighboring vessel formation, thereby facilitating the delivery of nutrients for cancer cell survival (Chen et al., 2017, Lian et al., 2019). Rivoceranib is an oral anti-angiogenic drug that highly selectively inhibits VEGFR-2 with a binding affinity 10 times higher than that of sorafenib or vantalanib (Hu et al., 2014; Yu et al., 2019). Previous studies have reported that rivoceranib inhibits VEGF-mediated tumor cell viability and migration via the VEGFR2/RAF/mitogen-activated protein kinase kinase (MEK)/extracellular signal-regulated kinase (ERK), and phosphoinositide 3-kinase (PI3K)/ AKT pathways (Huang et al., 2018).

Interestingly, our western blot analysis results showed that rivoceranib significantly reduced the activity of VEGFR2 *in vitro* and *in vivo* analysis. Furthermore, evidence of the rivoceranib-induced increase of TUNEL-positive MGT cells and fewer CD31-positive cells in treated than untreated tumor sections, led us to hypothesize that rivoceranib reduced cell viability and tumor angiogenesis by inhibiting VEGF/VEGFR2 signaling. However, these antitumor functions of rivoceranib still need to be confirmed in MGT canine patients. In conclusion, our results indicated that rivoceranib inhibited melanoma cell proliferation, migration, and cell cycle activities. The therapeutic efficacy of rivoceranib was also confirmed in a xenograft mouse model based on the increased apoptosis and inhibition of angiogenesis likely mediated via VEGFR2

signaling downregulation. These results suggest that rivoceranib may be a novel antiangiogenesis therapeutic strategy for canine MGTs that is worth further investigation.

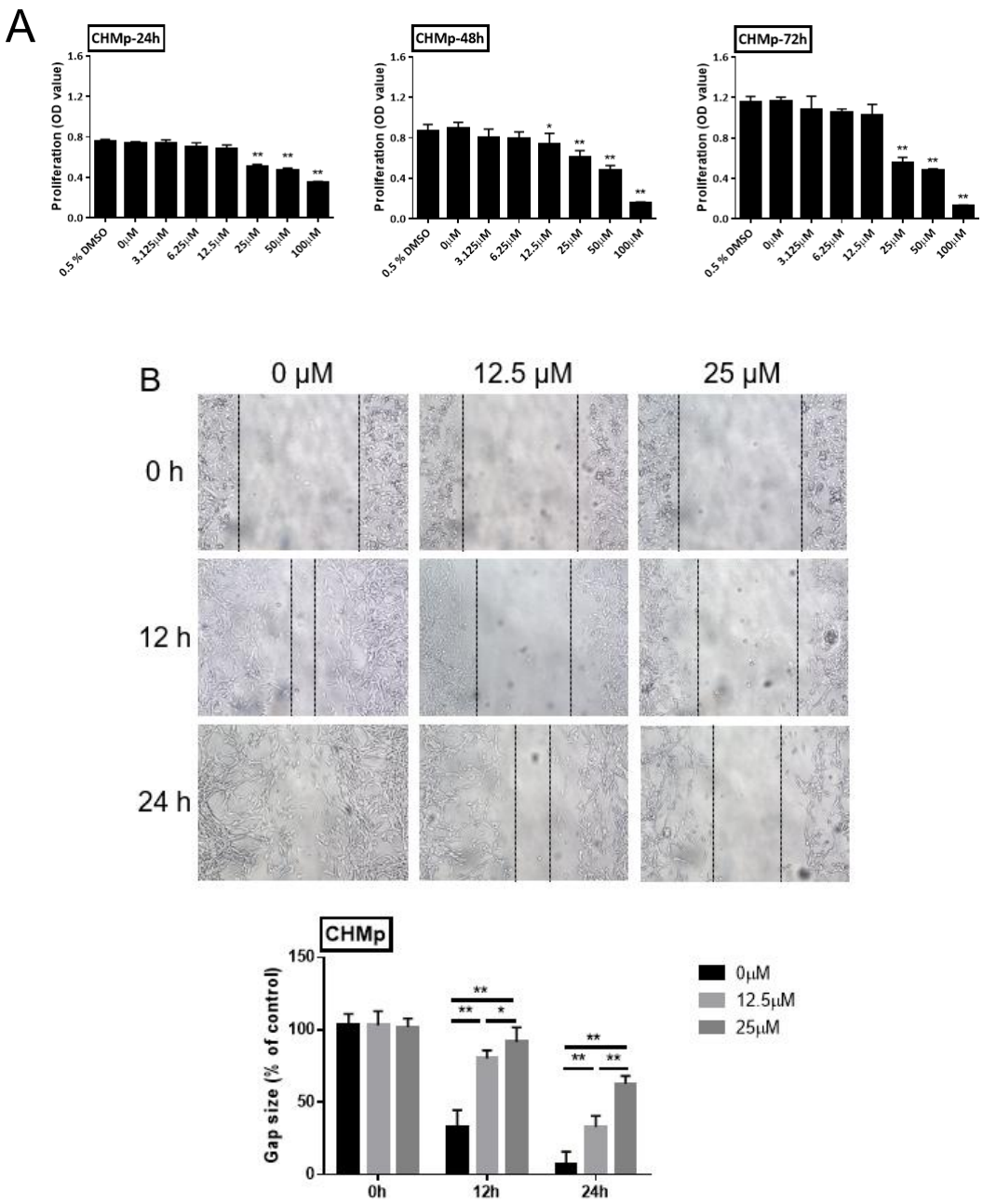

Figure 3.1. Effects of rivoceranib on cell proliferation and migration capacity *in vitro*. (A) Viability and (B) migration ability of CHMp cells treated with

varying concentrations of rivoceranib at 24, 48, and 72h. All experiments were performed in triplicate. Data are means ± standard deviation of three independent experiments. * $p < 0.05$ and ** $p < 0.01$ versus control group (0.5% dimethyl sulfoxide, DMSO) at same time point.

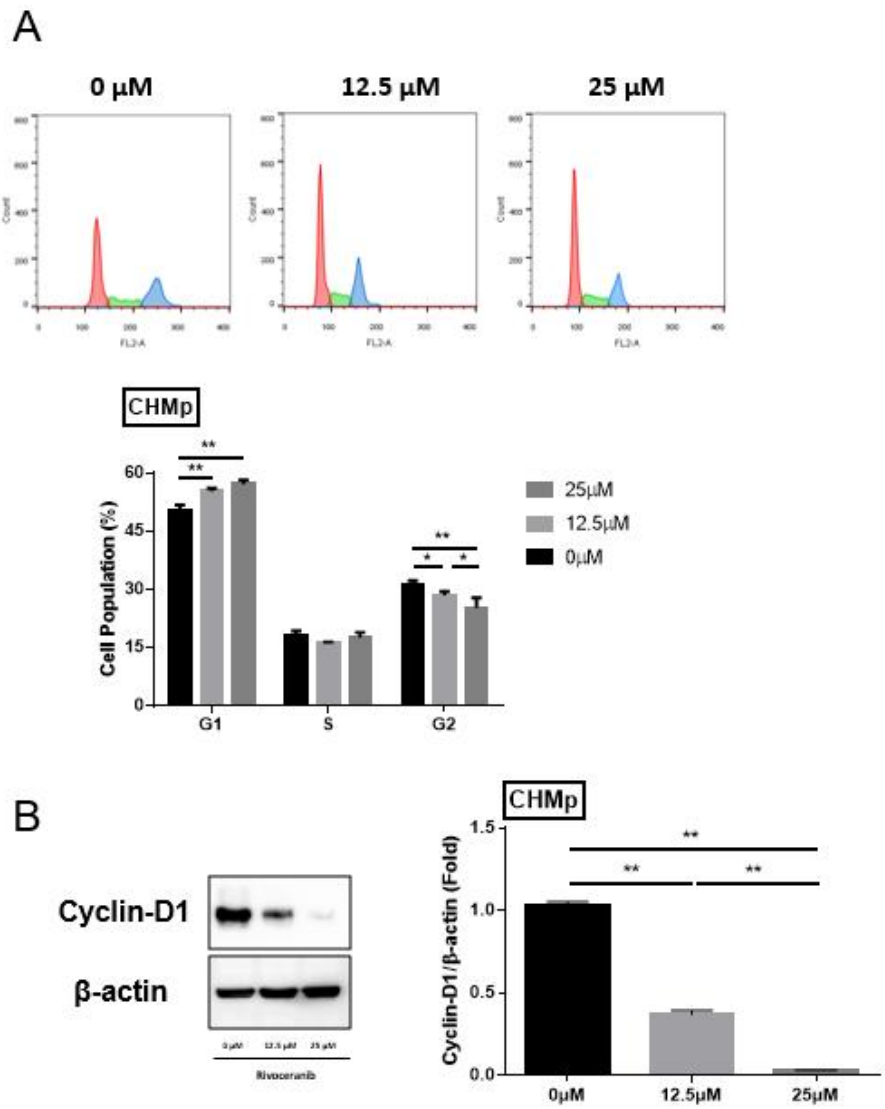

Figure 3.2. Effects of rivoceranib on cell cycle arrest *in vitro*. (A) Cell cycle distribution of CHMp cells treated with rivoceranib analyzed using flow cytometry at 48h. (B) Expression levels of cyclin D1 measured using western blotting. Band intensity on films presented as relative ratio of cyclin D1 to that of β-actin. Data are means ± standard deviation of three independent experiments. * $p < 0.05$ and ** $p < 0.01$.

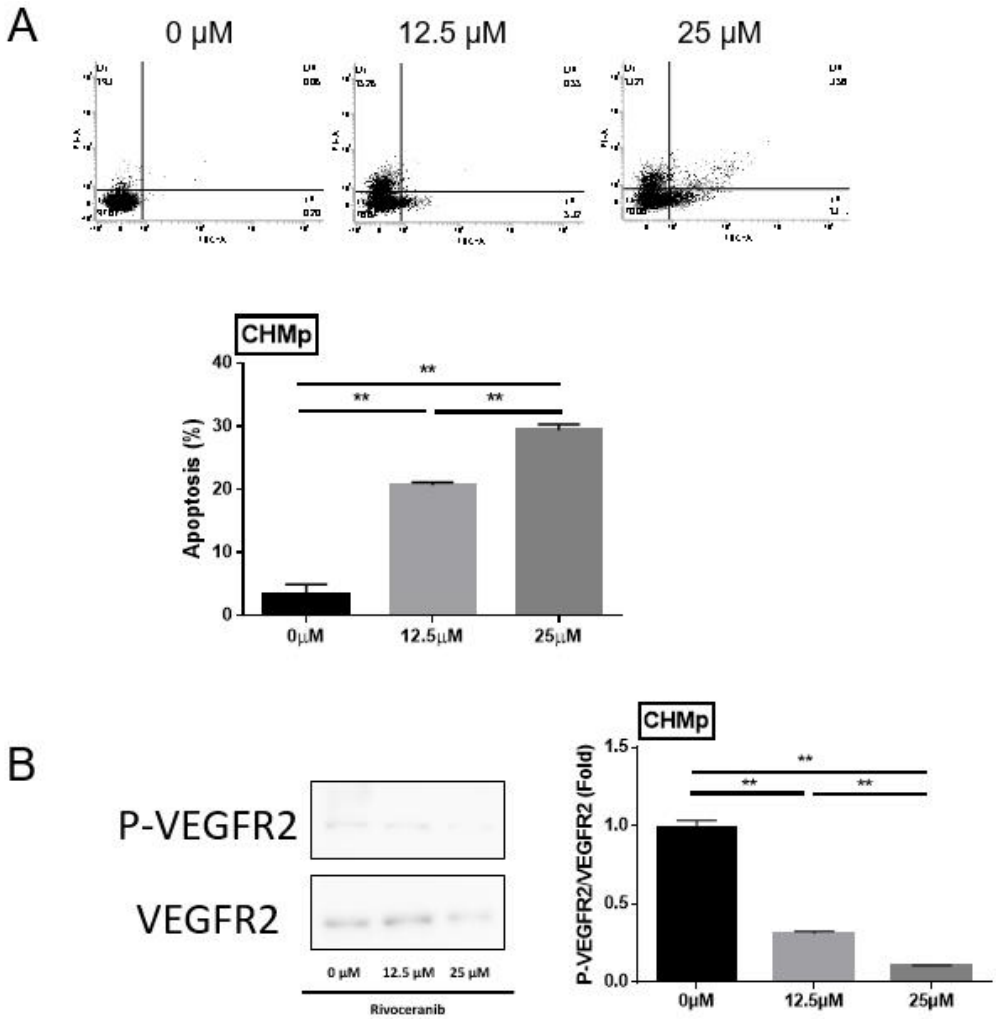

Figure 3.3. Effects of rivoceranib on CHMp cell apoptosis and vascular endothelial growth factor receptor 2 (VEGFR2) phosphorylation *in vitro*. (A) Apoptotic cell ratio was measured using flow cytometry. Apoptotic cells were quantified using Annexin V (fluorescein isothiocyanate [FITC]) and propidium iodide (PI [PE]) double-staining. (B) Activity of VEGFR2 was analyzed based on phosphorylation ratio using western blot. Band intensity on films presented as

relative ratio of p-VEGFR2 to that of VEGFR2. Data are means ± standard deviation of three independent experiments. ** $p < 0.01$.

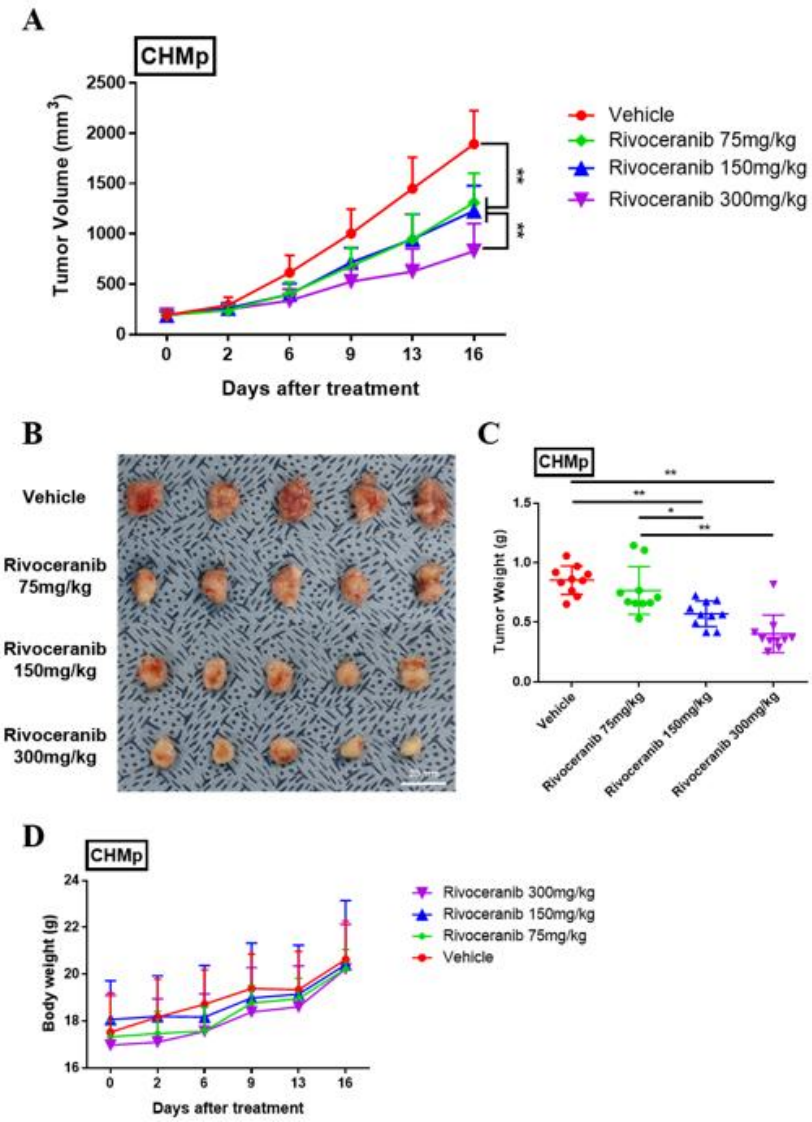

Figure 3.4. ***In vivo*** **effects of rivoceranib on xenograft model.** (A) Mean tumor volumes of four groups (vehicle and 75, 150, and 300 mg/kg rivoceranib-treated). (B) Representative images of collect tumors from xenograft model after 15 days of treatment. (C) Tumor weight were also measured. (D) Body weight of mice

monitored twice a week during rivoceranib treatment. Data are means ± standard deviation. * $p < 0.05$ and ** $p < 0.01$.

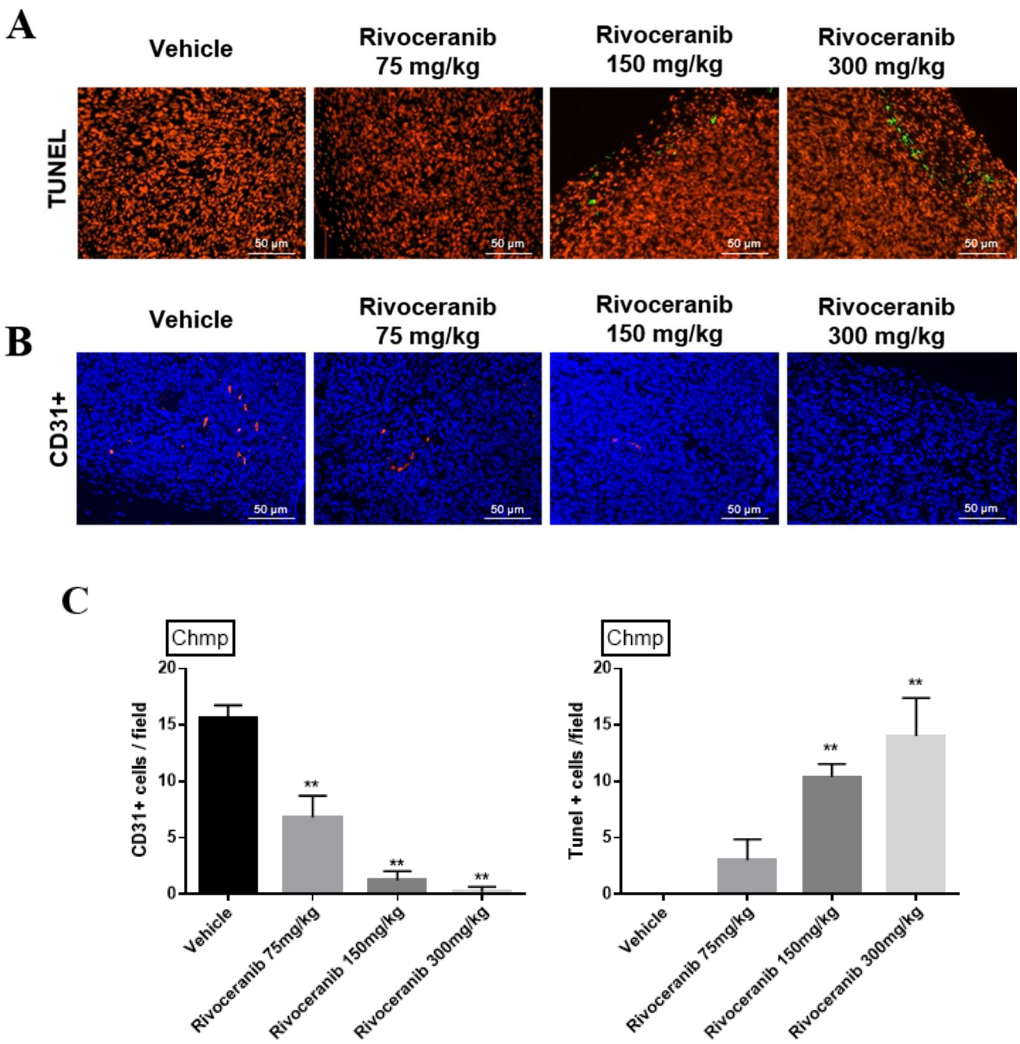

Figure 3.5. Effects of rivoceranib on apoptosis and angiogenesis *in vivo*. (A, B) Terminal deoxynucleotidyl transferase (TdT) deoxyuridine dUTP nick-end labeling (TUNEL) and anti-CD31 staining images of tumor sections from each group (vehicle and 75, 150, and 300 mg/kg rivoceranib). (C) TUNEL- and CD31-positive cells counted in six random fields per group under microscope (200×

magnification). Data are means ± standard deviation. ** $p < 0.01$ versus control (vehicle) group.

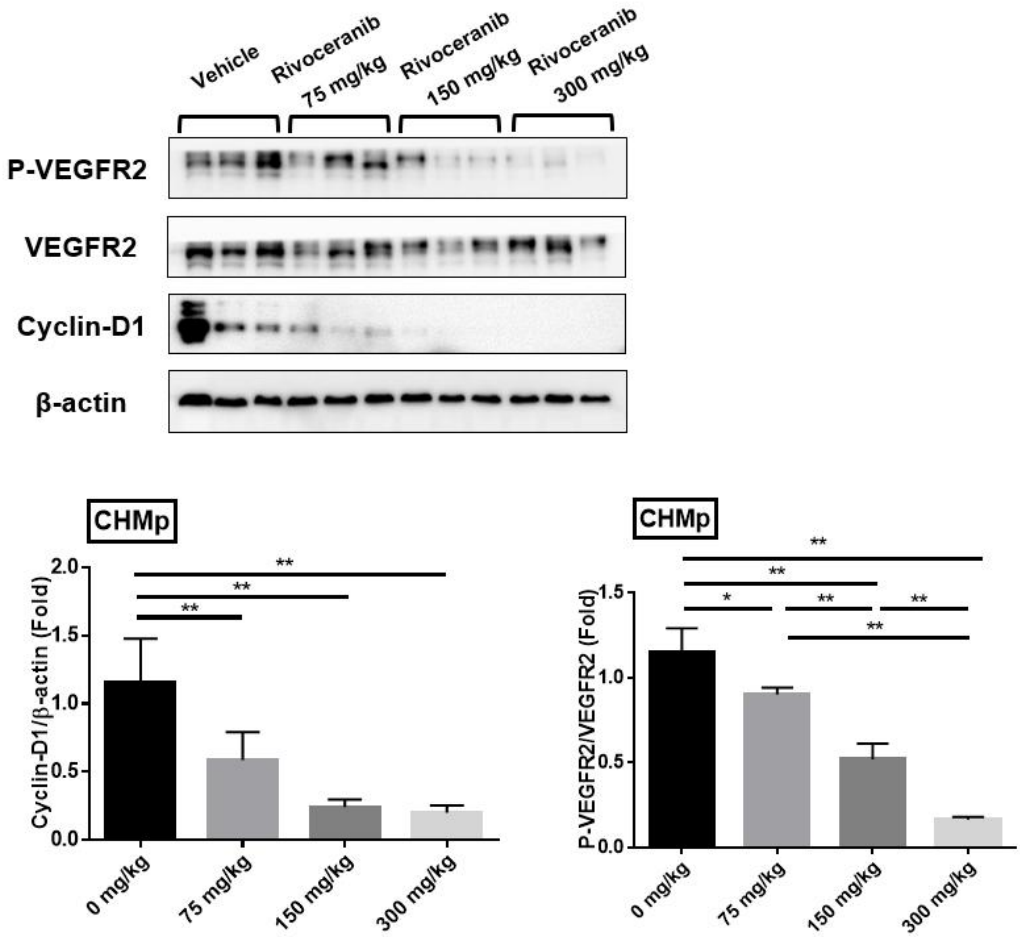

Figure 3.6. Effects of rivoceranib on protein levels of vascular endothelial factor receptor 2 (VEGFR2) phosphorylation and cyclin D1. Tumor tissue samples were analyzed using western blotting to evaluate of VEGFR2 activity and expression level of cyclin D1. Band intensities on films is presented as relative ratio of p-VEGFR2 to that of VEGFR2, and relative ratio of cyclin D1 to that of β-actin. Data are means ± standard deviation of three independent experiments. * $p < 0.05$ and ** $p < 0.01$.

GENERAL CONCLUSIONS

Rivoceranib, a VEGFR2 inhibitor, exhibits anti-tumor effects by targeting the microtubules in cancer cells. The objective of this study was to investigate the anti-tumor effects of rivoceranib *in vitro* and *in vivo*. To explore the underlying mechanism, tumor angiogenesis was examined by immunohistochemistry with an anti-CD31 antibody. Tumor cell apoptosis was detected by Tunnel assay, and cell cycle arrest was confirmed by western blot analysis. Rivoceranib treatment of canine melanoma and mammary gland tumor cells exerted mediated anti-proliferative effects and mediated cell cycle arrest *in vitro*. Summary, our results indicated that rivoceranib inhibits LMeC and CHMp cells proliferation, migration, and cell cycle activities. In animal experiments, also confirmed therapeutic efficacy in xenograft mouse models via increase apoptosis ratio and inhibit angiogenesis via VEGFR2 signaling downregulation. The results may suggest that rivoceranib may be novel anti-angiogenesis therapy strategy in canine tumors

REFERENCES

Abdelmegeed SM, Mohammed S. 2018. Canine mammary tumors as a model for human disease. *Oncology Letters*, 15, 8195-8205.

Almela RM, Ansón A. 2019. A Review of Immunotherapeutic Strategies in Canine Malignant Melanoma. *Veterianry Sciences*, 6, 15.

Ashman LK. 1999. The biology of stem cell factor and its receptor C-kit. *The International Journal of Biochemistry and Cell Biology*, 31, 1037-1051.

Banerjee S, Dowsett M, Ashworth A, Martin LA. 2007. Mechanisms of disease: angiogenesis and the management of breast cancer. *Nature Reviews Clinical Oncology*, 4, 53.

Blackwood L, Dobson JM, 1996. Radiotherapy of oral malignantmelanomas in dogs. *Journal of the American Veterinary Medical Association*, *209*, 98-102.

Breit MN, Kisseberth WC, Bear MD, Landesman Y, Kashyap T, McCauley D, Kauffman MG, Shacham S, London CA. 2014. Biologic activity of the novel orally bioavailable selective inhibitor of nuclear export (SINE) KPT-335 against canine melanoma cell lines. *BMC Veterinary Research*, 15, 160.

Brockley LK, Cooper MA, Bennett PF. 2013. Malignant melanoma in 63 dogs (2001-2011): The effect of carboplatin chemotherapy on survival. *New Zealand Vetetrinary Journal*, 61, 25-31.

Brodey RS. 1970. Canine and feline neoplasia. *Advances in Veterinary Science and Comparative Medicine*, 14, 309-354.

Cao CJ, Su Y, Sun J, Wang GY, Jia XQ, Chen HS, Xu AH. 2019. Anti-tumor Effect of Ginkgo biloba Exocarp Extracts on B16 Melanoma Bearing Mice Involving P I3K/Akt/HIF-1α/VEGF Signaling Pathways. *Iranian Journal of Pharmaceutical Research*, 18, 803-811.

Chen LT, Oh DY, Ryu MH, Yeh KH, Yeo W, Carlesi R, Cheng R, Kim J, Orlando M, Kang YK. 2017. Anti-angiogenic therapy in patients with advanced gastric and gastroesophageal junction cancer: a systematic review. *Cancer research and treatment: official journal of Korean Cancer Association*, 49, 851.

Cherrington JM, Strawn LM, Shawver LK. 2000. New paradigms for the treatment of cancer: the role of anti-angiogenesis agents. *Advances in Cancer Research*, 79, 1-38.

Clifford CA, de Lorimier LP, Fan T, Garrett LD. 2013. Muller and Kirk's Small Animal Dermatology 7th edition ISBN 978-1-4160-0028-0.

Cohen D, Reif JS, Brodey RS, Keiser H. 1974. Epidemiological analysis of the

most prevalent sites and types of canine neoplasia observed in a veterinary hospital. *Clinical Cancer Research*, 34, 2859-2868.

DE Campos CB, Lavalle GE, Monteiro LN, Pêgas GRA, Fialho SL, Balabram D, Cassali GD. 2018. Adjuvant Thalidomide and Metronomic Chemotherapy for the Treatment of Canine Malignant Mammary Gland Neoplasms. *In Vivo*, 32, 1659-1666.

Dervisis N, Klahn S. 2016. Therapeutic Innovations: Tyrosine Kinase Inhibitors in Cancer. *Veterinary Sciences*, 3.

DeSantis CE, Bray F, Ferlay J, Lortet-Tieulent J, Anderson BO, Jemal A. 2015. International variation in female breast cancer incidence and mortality rates. *Cancer Epidemiology, Biomarkers & Prevention*, 24, 1495-1506.

Druker BJ, Guilhot F, O'Brien SG, Gathmann I, Kantarjian H, Gattermann N, Deininger MW, Silver RT, Goldman JM, Stone RM, Cervantes F, Hochhaus A, Powell BL, Gabrilove JL, Rousselot P, Reiffers J, Cornelissen JJ, Hughes T, Agis H, Fischer T, Verhoef G, Shepherd J, Saglio G, Gratwohl A, Nielsen JL, Radich JP, Simonsson B, Taylor K, Baccarani M, So C, Letvak L, Larson RA. 2006. Five-year follow-up of patients receiving imatinib for chronic myeloid leukemia. *The new England Journal of Medicine*, 355, 2408-2417.

Ehrke MJ. 2003. Immunomodulation in cancer therapeutics. *International*

Immunopharmacology, 3, 1105-1119.

Eskens FA. 2004. Angiogenesis inhibitors in clinical development; where are we now and where are we going?, *British Journal of Cancer*, 90, 1-7.

Ewald F, Nörz D, Grottke A, Hofmann BT, Nashan B, Jücker M. 2014. Dual Inhibition of PI3K-AKT-mTOR-and RAF-MEK-ERK-signaling is synergistic in cholangiocarcinoma and reverses acquired resistance to MEK-inhibitors. *Investigational new drugs*, 32, 1144-1154.

Ferrara N, Gerber HP, LeCouter J. 2003. The biology of VEGF and its receptors. *Nature Medicine*, 9, 669-676.

Fletcher JA. 2004. Role of KIT and platelet-derived growth factor receptors as oncoproteins. *Seminars in Oncology*, 31, 4-11.

Fowles JS, Denton CL, Gustafson DL. 2015. Comparative analysis of MAPK and PI3K/AKT pathway activation and inhibition in human and canine melanoma. *Veterinary and Comparative Oncology*, 13, 288-304.

Reference 7- Gao Z, Shi M, Wang Y, Chen J, Ou Y. 2019. Apatinib enhanced anti-tumor activity of cisplatin on triple-negative breast cancer through inhibition of VEGFR-2. *Pathology-Research and Practice* , 215, 152422.

Ghoncheh M, Pournamdar Z, Salehiniya H. 2016. Incidence and mortality and epidemiology of breast cancer in the world. *Asian Pacific Journal of Cancer Prevention*, 17, 43-46.

Gogas HJ, Kirkwood JM, Sondak VK. 2007. Chemotherapy for metastatic melanoma: Time for a change?. *Cancer*, 109, 455-464.

Gray-Schopfer V, Wellbrock C, Marais R. 2007. Melanoma biology and new targeted therapy. *Nature*, 445, 851-857.

Haass NK, Smalley KS, Herlyn M. 2004. The role of altered cell-cell communication in melanoma progression. *Journal of Molecular Histology*, 35, 309-318.

Hall HI, Miller DR, Rogers JD, Bewerse B. 1999. Update on the incidence and mortality from melanoma in the United States. *Jornal of the American Academy of Dermatology*, 40, 35-42.

Hanahan D, Weinberg RA. 2000. The hallmarks of cancer. *Cell*, 100, 57-70.

Hanahan D, Weinberg RA. 2011. Hallmarks of cancer: the next generation. *Cell*, 144, 646-674.

Heath VL, Bicknell R. 2009. Anticancer strategies involving the vasculature. *Nature reviews Clinical oncology*, 6, 395.

Holmes K, Roberts OL, Thomas AM, Cross MJ. 2007. Vascular endothelial growth factor receptor-2: structure, function, intracellular signalling and therapeutic inhibition. *Cellular signalling*, 19, 2003-2012.

Huang M, Huang B, Li G, Zeng S. 2018. Apatinib affect VEGF-mediated cell proliferation, migration, invasion via blocking VEGFR2/RAF/MEK/ERK

and PI3K/AKT pathways in cholangiocarcinoma cell. *BMC gastroenterology*, 18, 169.

Hu X, Cao J, Hu W, Wu C, Pan Y, Cai L, Tong Z, Wang S, Li J, Wang Z, Wang B, Chen X, Yu H. 2014. "Multicenter phase II study of apatinib in non-triple-negative metastatic breast cancer. *BMC cancer*, 14, 820.

Igase M, Hwang CC, Kambayashi S, Kubo M, Coffey M, Miyama TS, Baba K, Okuda M, Noguchi S, Mizuno T. 2016. Oncolytic reovirus synergizes with chemotherapeutic agents to promote cell death in canine mammary gland tumor. *Canadian Journal of Veterinary Research*, 80, 21-31.

Inoue K, Ohashi E, Kadosawa T, Hong SH, Matsunaga S, Mochizuki M, Nishimura R, Sasaki N. 2004. Establishment and Characterization of Four Canine Melanoma Cell Lines. *The Journal of Veterinary Medical Science*, 29, 181-183.

Kang Y, Lee KH, Shen L, Yeh K, Hong Y, Park YI, Yang SH, Shin DB, Zang DY, Kang WK, Chung IJ, Kim YH, Ryoo B, Park SR, Nam B, Ryu MH. 2014. 615O Randomized phase II study of capecitabine and cisplatin with or without sorafenib in patients with metastatic gastric cancer: stargate study. *Annals of Oncology*, 25, iv210.

Kimura KC, Gárate AP, Dagli M. 2012. Retrospective study of neoplasms in domestic animals: A survey between 1993 and 2002 of the Service of

Animal Pathology, Department of Pathology, School of Veterinary Medicine and Animal Science, University of Sao Paulo, Southeast Brazil. *Brazilian Journal of Veterinary Pathology*, 5, 60-69.

Karasic TB, Rosen MA, O'Dwyer PJ. 2017. Antiangiogenic tyrosine kinase inhibitors in colorectal cancer: is there a path to making them more effective?. *Cancer Chemotherapy and Pharmacology*, 80, 661–71.

Kerbel RS. 2006. Antiangiogenic therapy: a universal chemosensitization strategy for cancer?. *Science*, 26, 1171-1175.

Kowanetz M, Ferrara N. 2006. Vascular endothelial growth factor signaling pathways: therapeutic efficacy. *Clinical Cancer Research*, 12, 5018–5022.

La-Beck NM, Jean GW, Huynh C, Alzghari SK, Lowe DB. 2015. Immune Checkpoint Inhibitors: New In-sights and Current Place in Cancer Therapy. *Pharmacotherapy*, 35, 963–976.

Langer CJ, Mok T, Postmus PE. 2013. Targeted agents in the third-/fourth-line treatment of patients with advanced (stage III/IV) non-small cell lung cancer (NSCLC). *Cancer Treatment Reviews*, 39, 252-260.

Laskin JJ, Sandler AB. 2004. Epidermal growth factor receptor: a promising target in solid tumours. *Cancer Metastasis Reviews*, 30, 1-17.

Lee JH, Li Q, An JH, Chae HK, Choi JW, Kim BJ, Song WJ, Youn HY. 2019. Antitumor Activity of Rivoceranib Against Canine Mammary Gland

Tumor Cell Lines. *Anticancer Research*, 39, 5483-5494.

Li J, Qin S, Xu J, Guo W, Xiong J, Bai Y, Sun G, Yang Y, Wang L, Xu N, Cheng Y, Wang Z, Zheng L, Tao M, Zhu X, Ji D, Liu X, Yu H. 2013. Apatinib for chemotherapy-refractory advanced metastatic gastric cancer: results from a randomized, placebo-controlled, parallel-arm, phase II trial. *Journal of Clinical Oncology*, 10, 3219-3225.

Li J, Qin S, Xu J, Xiong J, Wu C, Bai Y, Liu W, Tong J, Liu Y, Xu R, Wang Z, Wang Q, Ouyang X, Yang Y, Ba Y, Liang J, Lin X, Luo D, Zheng R, Wang X, Sun G, Wang L, Zheng L, Guo H, Wu J, Xu N, Yang J, Zhang H, Cheng Y[1], Wang N, Chen L, Fan Z, Sun P, Yu H. 2016. Randomized, double-blind, placebocontrolled phase III trial of apatinib in patients with chemotherapy-refractory advanced or metastatic adenocarcinoma of the stomach or gastroesophageal junction. *Journal of Clinical Oncology*, 34, 1448–1454.

Li J, Zhao X, Chen L, Guo H, Lv F, Jia K, Yv K, Wang F, Li C, Qian J, Zheng C, Zuo Y. 2010. Safety and pharmacokinetics of novel selective vascular endothelial growth factor receptor-2 inhibitor YN968D1 in patients with advanced malignancies. *BMC cancer*, 10, 529.

Lian L, Li XL, Xu MD, Li XM, Wu MY, Zhang Y, Tao M, Li W, Shen XM, Zhou C, Jiang M. 2019. VEGFR2 promotes tumorigenesis and metastasis in a

pro-angiogenic-independent way in gastric cancer. *BMC cancer*, 19, 183.

Liao J, Jin H, Li S, Xu L, Peng Z, Wei G, Long J, Guo Y, Kuang M, Zhou Q, Peng S. 2019. Apatinib potentiates irradiation effect via suppressing PI3K/AKT signaling pathway in hepatocellular carcinoma. *Journal of Experimental & Clinical Cancer Research,* 38, 454.

London CA. 2009. Tyrosine kinase inhibitors in veterinary medicine. *Topics in Companion Animal Medicine*, 24, 106-112.

London CA, Hannah AL, Zadovoskaya R, Chien MB, Kollias-Baker C, Rosenberg M, Downing S, Post G, Boucher J, Shenoy N, Mendel DB, McMahon G, Cherrington JM. 2003. Phase I dose-escalating study of SU11654, a small molecule receptor tyrosine kinase inhibitor, in dogs with spontaneous malignancies. *Clinical Cancer Research*, 9, 2755-2768.

Madhusudan S, Ganesan TS. 2004. Tyrosine kinase inhibitors in cancer therapy. *Clinical Biochemistry*, 37, 618-635.

Ma PC, Maulik G, Christensen J, Salgia R. 2003. c-Met: structure, functions and potential for therapeutic inhibition. *Cancer Metastasis Reviews*, 22, 309-325.

McCarty MF, Liu W, Fan F, Parikh A, Reimuth N, Stoeltzing O, Ellis LM. 2003. Promises and pitfalls of anti-angiogenic therapy in clinical trials. *Trends in Molecular Medicine*, 9, 53-58.

Mellman, I.; Coukos, G.; Dranoff, G. 2011. Cancer immunotherapy comes of age. *Nature*, 7378, 480–489.

Mitchell L, Thamm DH, Biller BJ. 2012. Clinical and immunomodulatory effects of toceranib combined with low-dose cyclophosphamide in dogs with cancer. *Journal of Veterinary Internal Medicine*, 26, 355-362.

Moe L. 2001. Population-based incidence of mammary tumours in some dog breeds. *Journal of Reproduction of Fertility. Supplement*,57, 439-443.

Martin V. 1993. Overview of paclitaxel (TAXOL). *Semin Oncol Nurs*, 9, 2-5.

Reference 30- Moehler M, Mueller A, Hartmann JT, Ebert MP, Al-Batran SE, Reimer P, Weihrauch M, Lordick F, Trarbach T, Biesterfeld S, Kabisch M, Wachtlin D, Galle PR. 2011. An open-label, multicentre biomarker-oriented AIO phase II trial of sunitinib for patients with chemo-refractory advanced gastric cancer. *European Journal of Cancer*, 47, 1511-1520.

Neubauer A, Burchert A, Maiwald C, Gruss HJ, Serke S, Huhn D, Wittig B, Liu E. 1997. Recent progress on the role of Axl, a receptor tyrosine kinase, in malignant transformation of myeloid leukemias. *Leukemia & Lymphoma*, 25, 91-96.

Nishiya AT, Massoco CO, Felizzola CR, Perlmann E, Batschinski K, Tedardi MV, Garcia JS, Mendonça PP, Teixeira TF, Zaidan Dagli ML. 2016.

Comparative Aspects of Canine Melanoma. *Veterinary Sciences*. 19, pii: E7.

Novosad CA: Principles of treatment for mammary gland tumors. 2003. *Clinical Techniques in Small Animal Practice*, 18, 107-109.

Nishida N, Yano H, Nishida T, Kamura T, Kojiro M. 2006. Angiogenesis in cancer.*Vascular Health and Risk Management*, 2, 213-219.

Panchagnula R. 1998. Pharmaceutical aspects of paclitaxel. *International Journal of Pharmaceutics*, 172, 1-15.

Paul MK, Mukhopadhyay AK. 2004. Tyrosine kinase - Role and significance in Cancer. *International Journal of Medical Sciences*, 1, 101-115.

Peng H, Zhang Q, Li J, Zhang N, Hua Y, Xu L, Deng Y, Lai J, Peng Z, Peng B, Chen M, Peng S, Kuang M. 2016. Apatinib inhibits VEGF signaling and promotes apoptosis in intrahepatic cholangiocarcinoma. *Oncotarget*, 29, 17220-17229.

Philibert JC, Snyder PW, Glickman N, Glickman LT, Knapp DW, Waters DJ. 2003. Influence of host factors on survival in dogs with malignant mammary gland tumors. *Journal of Veterianry Internal Medicine*, 17, 102-106.

Pierini A, Bocci G, Giorgi M, Owen H and Marchetti V. 2012. From humans to dogs and back: The translational lesson of metronomic chemotherapy.

American Journal of Animal and Veterinary Sciences, 7, 198-212.

Pinto MP, Owen GI, Retamal I, Garrido M. 2017. Angiogenesis inhibitors in early development for gastric cancer. *Expert Opinion on Investigational Drugs*, 26, 1007–1017.

Qin S. 2014. Phase III study of apatinib in advanced gastric cancer: A randomized, double-blind, placebo-controlled trial, *Journal of Clinical Oncology*, 4003.

Qin S, Li A, Yi M, Yu S, Zhang M, Wu K. Recent advances on anti-angiogenesis receptor tyrosine kinase inhibitors in cancer therapy. *Jornal of Hematology & Oncology*, 12, 27.

Quintin-Colonna, F., Devauchelle, P., Fradelizi, D., Mourot, B., Faure, T., Kourilsky, P., Roth, C., and Mehtali, M. 1996. Gene therapy of spontaneous canine melanoma and feline fibrosarcoma by intratumoral administration of histoincompatible cells expressing human interleukin-2. *Gene Therapy*, 3, 1104-1112.

Raje N, Anderson KC. 2002. Thalidomide and immunomodulatory drugs as cancer therapy. *Current Opinion in Oncology*, 14, 635-640.

Rapisarda A, Melillo G. 2009. Role of the hypoxic tumor microenvironment in the resistance to anti-angiogenic therapies. *Drug Resistance Updates*, 12, 74-80

Roviello G, Petrioli R, Marano L, Polom K, Marrelli D, Perrella A, Roviello F.

2016. Angiogenesis inhibitors in gastric and gastroesophageal junction cancer, *Gastric Cancer,* 19, 31–41.

Roviello G, Ravelli A, Polom K, Petrioli R, Marano L, Marrelli D, Roviello F, Generali D. 2016. Apatinib: A novel receptor tyrosine kinase inhibitor for the treatment of gastric cancer. *Cancer Letters*, 28, 187-191.

Rutteman GR, Erich SA, Mol JA, Spee B, Grinwis GC, Fleckenstein L, London CA, Efferth T. 2013. Safety and efficacy field study of artesunate for dogs with non-resectable tumours. *Anticancer Research*, 33, 1819-1827.

Schiffer CA. 2001. Signal transduction inhibition: Changing paradigms in cancer care. *Seminars in Oncology*, 28, 34–39.

Scott LJ. 2018. Apatinib: A Review in Advanced Gastric Cancer and Other Advanced Cancers. *Drugs*, 78, 747-758.

Siemann DW, Chaplin DJ, Horsman MR. 2017. Realizing the potential of vascular targeted therapy: the rationale for combining vascular disrupting agents and anti-angiogenic agents to treat cancer. *Cancer Investigation*, 35, 519–534.

Simon D, Schoenrock D, Baumgärtner W, Nolte I. 2006. Postoperative adjuvant treatment of invasive malignant mammary gland tumors in dogs with doxorubicin and docetaxel. *Journal of Veterinary Internal Medicine*, 20, 1184-90.

Sorenmo KU. 2003. Canine mammary gland tumors. *Veterinary Clinics of North America Small Animal Practice,* 33: 573-596.

Sorenmo KU, Worley DR, Goldschmidt MH. 2013. Withrow & MacEwen's Small Animal Clinical Oncology. 5th edition.

Spangler WL, Kass PH. 2006. The histologic and epidemiologic bases for prognostic considerations in canine melanocytic neoplasia. *Veterinary Pathology*, 43, 136-149.

Stephen J, David M. Vail, Rodney L Page. 2013. Withrow and Macewen's Small animal clinical oncology 5th edition ISBN: 978-1-4377-2362-5 Copyright©.

Stephens T. 2019. The Use of Chemotherapy to Prolong the Life of Dogs Suffering from Cancer: The Ethical Dilemma. *Animals (Basel)*, 14.

Sweet M, Kirkham N, Bendall M, Currey L, Bythell J, Heupel M. 2012. Evidence of Melanoma in Wild Marine Fish Populations. *PLoS One*, 7, e41989.

Taylor ML, Metcalfe DD. 2000. Kit signal transduction. *Hematology Oncology Clinics of North America*, 14, 517-535.

Teixeira TF, Da TC, 2010. Cogliati B, Nagamine MK. Retrospective study of melanocytic neoplasms in dogs and cats. *Brazil Journal of Veterinay Pathology*, 3, 100-104.

Thurston G, Gale NW. 2004. Vascular endothelial growth factor and other

signaling pathways in developmental and pathologic angiogenesis. *International Journal of Hematology*, 80, 7-20.

Todoroff RJ, Brodey RS. 1979. Oral and pharyngeal neoplasia in the dog: a retrospective survey of 361 cases. *Journal of the American Veterinary Med Association*, 175, 567-571.

Traxler P, Bold G, Buchdunger E, Caravatti G, Furet P, Manley P, O'Reilly T, Wood J, Zimmermann J. 2001. Tyrosine kinase inhibitors: from rational design to clinical trials. *Medical Research Reviews*. 21, 499-512.

Weaver BA. 2014. How Taxol/paclitaxel kills cancer cells. *Molecular Biology of the Cell*, 25, 2677-2681.

Weinstock MA. 1997. Death From Skin Cancer Among the Elderly. *Archives of Dermatoogyl*, 133, 12071209.

Yu GC, Yang J, Ye B, Xu LL, Li XY, Zheng GR. 2019. Apatinib in the treatment of advanced non-small-cell lung cancer: A meta-analysis. *Mathematical biosciences and engineering,* 21, 7659-7670.

Zhang Q, Song Y, Cheng X, Xu Z, Matthew OA, Wang J, Sun Z, Zhang X. 2019. Apatinib Reverses Paclitaxel-resistant Lung Cancer Cells (A549) Through Blocking the Function of ABCB1 Transporter. *Anticancer Research*, 39, 5461-5471.

Zsebo KM, Williams DA, Geissler EN, Broudy VC, Martin FH, Atkins HL, Hsu

RY, Birkett NC, Okino KH, Murdock DC. 1990. Stem cell factor is encoded at the Sl locus of the mouse and is the ligand for the c-kit tyrosine kinase receptor. *Cell*, 5, 213-224.

Zwick E, Bange J, Ullrich A. 2002. Receptor tyrosine kinases as targets for anticancer drugs. *Trends in Molecular Medicine*, 8, 17-23.

Zhang Z, Zhao Y, Lu F, Hou X, Ma Y, Luo F, Zeng K, Zhao S, Zhang Y[1], Zhou T, Yang Y, Fang W, Huang Y, Zhang L, Zhao H. 2019. Multi-targeted tyrosine kinase inhibitors as third-line regimen in advanced non-small cell lung cancer: a network meta-analysis. *Annals of Translational Medicine*, 7, 452.

국 문 초 록

개의 악성 흑색종 및 유선암에서 Tyrosine Kinase Inhibitor인 Rivoceranib의 항종양 효과

김유석

(지도교수 윤화영)

서울대학교 대학원

수의과대학 임상수의학 (수의내과학) 전공

암은 반려견의 주요 사망원인 중의 하나로 10세령 이상의 개의 50% 이상에서 적어도 1가지 이상의 악성 종양에 거리는 것으로 알려

져 있으며 (London et al., 2003), 미국에서는 암이 2세 이상의 개에서는 사망의 원인이 되는 것으로 보고되었다 (Stephens et al., 2019)

이렇듯 개에서 암이 빈번히 발생하고 죽음의 원인되는 상황을 고려할 때 인의 및 수의학에서, 표준 요법에 반응하지 않는 종양에 대해 치료 반응을 보이는 novel한 항종양 악물이 시급이 요구되는 상황이다. (Rutteman et al., 2013).

Tyrosine kinase는 tyrosine residue의 다른 단백질을 인산화 시키는 단밸질로 세포 성장과 분화 조절에 긴밀하게 작용하는 정상 세포 신호 전달 체계에서 중요한 역할을 한다. VEGFR은 혈관 내피세포에서 발현하며, VEGF-VEGFR 상호작용은 내피세포의 이주와 증식에 중요한 역할을 한다. (Thurston G et al., 2004). PDGF와 PDGFR은 기질과 pericyte에서 발현되며, PDGF는 혈관신생을 촉진할 수 있다. (London., 2009, Cherrington JM et al., 2000, McCarty MF et al., 2003).

Angiogenesis는 악성 종양 연구에서 major scientific interest의 주제로 생각되고 있다. 최근 anti-angiogenic small molecule receptor tyrosine kinase inhibitors (TKIs) 등을 포함한 여러 혈관신생 타겟의 약물이 다양한 carcinoma에서 성공을 거두고 있다. (Qin et al., 2019)

이렇듯 사람의 종양 연구에서는 tyrosine kinase의 이상에 대한

연구가 많이 진행되어 있으나, 수의 종양학에서는 연구가 비교적 덜 되어 있는 상황이다. (London., 2009).

Rivoceranib은 VEGFR2 inhibitor로 암세포의 microtubule을 타겟하여 항종양 효과를 발휘한다. 최근에 사람 암환자에서 종양의 개선효과가 있음이 보고되었다. 이에 본 연구는 rivoceranib의 *in vitro* 및 *in vivo* 실험을 통해 개의 흑색종 (LMeC) 및 유선종양 (CHMp) 세포에서의 항암 효과를 확인하고자 진행하였다.

세포독성 평가 결과 약물 48h 적용시 LMeC 및 CHMp에서 각각 6.25, 12.5uM부터 나타나기 시작했다. 또한 약물 처리 농도의 증가에 따라 세포성장이 감소하는 양상을 확인할 수 있었다. 이러한 성장 억제 및 세포독성에 대한 기전 확인을 위하여 세포주기분석 (Cell cycle analysis), 세포사멸분석 (Cell apoptosis analysis) 및 단백질발현 (Western blot) 분석을 진행하였으며, 그 결과 주로 암세포주의 G1기 arrest를 통한 세포 분열 억제, 사멸 및 괴사세포의 증가 및 VEGFR2 단백질 활성 억제를 통해 해당 세포독성 효과가 나타나는 것으로 확인되었다.

또한 LMeC 및 CHMp가 이식된 마우스 종양모델을 이용하여 xenograft 실험을 진행하였으며, Rivoceranib을 75, 150 및

300mg/kg로 LMeC 모델에서는 28일간, CHMp 모델에서는 15일간 각각 일일 1회 경구투여 하였다.

그 결과 LMeC 모델에서는 150mg/kg 및 300mg/kg 투여 그룹에서 vehicle 그룹 대비 유의적인 종양 크기 감소가 확인되었으며, CHMp 모델에서는 모든 용량에서 vehicle 그룹 대비 종양의 크기가 유의적으로 감소하였다. 또한 부검 시 적출한 종양의 무게 측정에서도 투여된 약물의 농도 의존적으로 종양 무게가 감소된 것을 확인하였다.

또한 부검 시 적출한 종양조직의 분석 결과 역시 RIVOCERANIB은 세포 사멸 유도, 세포분열 억제, 종양 혈관화 능력을 억제함을 확인할 수 있었다.

본 시험은 개의 melanoma와 mammary gland tumor에 대해 Tyrosine Kinase Inhibitor인 Rivoceranib의 항암 치료 효과를 처음으로 진행한 연구이며, 본 결과를 통해 개의 종양 환자에서 Rivoceranib을 항암제로 적용해볼 수 있는 가능성이 확인되었다.

주요어: 개 / 흑색종 / 유선종양 / Rivoceranib / VEGFR2

학번: 2016-36632